Magnetic black holes and monopoles in a nonminimal Einstein-Yang-Mills theory with a cosmological constant: Exact solutions

Alexander B. Balakin,[1,*] José P. S. Lemos,[2,†] and Alexei E. Zayats[1,‡]

[1] *Department of General Relativity and Gravitation, Institute of Physics, Kazan Federal University, Kremlevskaya str. 18, Kazan 420008, Russia*

[2] *Centro Multidisciplinar de Astrofísica-CENTRA, Departamento de Física, Instituto Superior Técnico-IST, Universidade de Lisboa-UL, Avenida Rovisco Pais 1, 1049-001 Lisboa, Portugal*

arXiv:1603.02676v2 [gr-qc] 4 Apr 2016

Alternative theories of gravity and their solutions are of considerable importance since at some fundamental level the world can reveal new features. Indeed, it is suspected that the gravitational field might be nonminimally coupled to the other fields at scales not yet probed, bringing into the forefront nonminimally coupled theories. In this mode, we consider a nonminimal Einstein-Yang-Mills theory with a cosmological constant. Imposing spherical symmetry and staticity for the spacetime and a magnetic Wu-Yang ansatz for the Yang-Mills field, we find expressions for the solutions of the theory. Further imposing constraints on the nonminimal parameters, we find a family of exact solutions of the theory depending on five parameters, namely, two nonminimal parameters, the cosmological constant, the magnetic charge, and the mass. These solutions represent magnetic monopoles and black holes in magnetic monopoles with de Sitter, Minkowskian, and anti-de Sitter asymptotics, depending on the sign and value of the cosmological constant Λ. We classify completely the family of solutions with respect to the number and the type of horizons and show that the spacetime solutions can have, at most, four horizons. For particular sets of the parameters, these horizons can become double, triple, and quadruple. For instance, for a positive cosmological constant Λ, there is a critical Λ_c for which the solution admits a quadruple horizon, evocative of the Λ_c that appears for a given energy density in both the Einstein static and Eddington-Lemaître dynamical universes. As an example of our classification, we analyze solutions in the Drummond-Hathrell nonminimal theory that describe nonminimal black holes. Another application is with a set of regular black holes previously treated.

PACS numbers: 04.20.Jb, 04.40.Nr, 14.80.Hv

I. INTRODUCTION

There is great interest in finding compact objects and black hole solutions in all possible viable gravitational theories, from general relativity coupled minimally to all forms of matter, to alternative theories of gravitation such as nonminimally coupled theories.

Vacuum spherically symmetric general relativity contains the Schwarzschild black hole, and when coupled minimally to the Maxwell electromagnetic field, contains the Reissner-Nordström black hole, see e.g., [1]. When coupled to the Yang-Mills field, spherically symmetric general relativity yields soliton [2] and black hole solutions [3] with Yang-Mills hair, and the addition of a Higgs field produces remarkable magnetic monopole black holes [4–6]. There are many other solutions. For instance, compact objects and black holes appear in a non-Abelian Born-Infeld theory coupled to general relativity [7] and in supersymmetric Einstein-Yang-Mills theories [8]. In addition, regular black holes, i.e, nonsingular black holes that have special features, also show up when general relativity is coupled minimally to other fields [9–13]. Vacuum rotating stationary general relativity contains the Kerr black hole, and when coupled minimally to the Maxwell electromagnetic field, contains the Kerr-Newman black hole, see, e.g., [1]. Some of the spherically symmetric solutions mentioned above also have their counterpart when put to rotate. To add a cosmological constant to the general relativity equations gives, in pure vacuum, the de Sitter (dS) solution and the anti-de Sitter (AdS) solution, depending on whether the cosmological constant is positive or negative, respectively. In such a case, the massive solutions are enlarged to the Schwarzschild-dS solution or the Schwarzschild-AdS solution, depending on whether the cosmological constant is positive or negative, respectively, and the corresponding generalizations when one includes electric or magnetic charge and rotation [1]. Non-Abelian monopole solutions in dS spacetimes have been found in [14] and black hole hairy solutions for a Yang-Mills field coupled to spherically symmetric general relativity in AdS spacetimes have also been found [15–17].

Differently from minimally coupled fields, there are theories that couple the gravitational field to other fields using cross terms containing the curvature tensor. One says then that the theory is nonminimally coupled. There are many fields which can be nonminimally coupled to gravitation. For instance, the electromagnetic field is nonminimally coupled to the gravitational field in [18–20].

*Electronic address: Alexander.Balakin@kpfu.ru
†Electronic address: joselemos@ist.utl.pt
‡Electronic address: Alexei.Zayats@kpfu.ru

In nonminimally coupled theories spherically symmetric solutions with an electric field have been found in [21–23], including black holes [24] and wormholes [25]. Solutions with a magnetic field of the Wu-Yang type in a Yang-Mills theory nonminimally coupled to the gravitational field have been found as monopoles in [26, 27], as wormholes in [28, 29], and as regular black holes in [30].

Here we want to proceed with the studies initiated in [26–28] and find nonminimal solutions, now with a generic cosmological constant (see also [29] for wormhole solutions with a cosmological constant). Indeed, we find a general set of magnetic monopoles and black holes with positive, zero, and negative cosmological constant of which the regular black holes found in [30] are a small subset.

The nonminimal theory we use is provided in [20], and its extension from a Maxwell to a Yang-Mills field is in [26]. In addition to the Einstein-Hilbert term and to the Yang-Mills term, the theory couples the Yang-Mills field linearly to a nonminimal susceptibility tensor in which three parameters q_1, q_2, and q_3, appear as coefficients in front of the Ricci scalar, Ricci tensor and Riemann tensor, respectively. These three parameters can be considered phenomenological and have units of length square.

We put in the theory, and thus in the action, a cosmological Λ term, which has units of inverse length square. A positive cosmological term appears in a cosmological framework for providing the acceleration of the Universe and as a setting for the dark energy. It also appears in black hole physics. First, regular black holes need some kind of positive cosmological constant in its interior to provide enough repulsion that does not allow a singularity formation (see, e.g., [11]). Second, a generic cosmological constant, positive, zero, or negative gives spacetimes that are asympotically dS, Minkowski, or AdS. The first case is the Universe in which we live, the second case is mathematically simpler with good asymptotic properties, and the third might be a world for elementary particles as predicted in supergravity theories.

In considering solutions describing nonminimal magnetic monopole stars and nonminimal magnetic black holes we aim to construct fully exact solutions from the origin to infinity without the need of a matching boundary. Clearly it is an important task to find continuous black hole solutions for which no junction is needed. We find that nonminimal coupled theories of a Yang-Mills field with a Wu-Yang ansatz in spherically symmetric static spacetime yields such solutions. The Wu-Yang ansatz in such a spacetime provides a magnetic parameter ν for the Yang-Mills field, or its square $Q_m^2 = 4\pi\nu^2$ giving the magnetic charge Q_m. The gravitational equations give the mass parameter M.

It is reasonable to restrict our quest, as we do, by imposing some asymptotic conditions at large values of the radial variable r. We assume that at r large one should obtain a magnetic Reissner-Nordström-dS solution, a magnetic Reissner-Nordström solution, or a magnetic Reissner-Nordström-AdS solution. Generically the magnetic Reissner-Nordström solution with a cosmological constant is $ds^2 = N(r)dt^2 - \frac{dr^2}{N(r)} - r^2\left(d\theta^2 + \sin^2\theta d\varphi^2\right)$, where the metric function $N(r)$ is of the form $N(r) = 1 - \frac{2M}{r} + \frac{Q_m^2}{r^2} - \frac{\Lambda}{3}r^2$. Here Q_m is the magnetic charge, that can be also an electric charge, and M is the asymptotic mass of the object. At $r \to \infty$ it has a dS asymptote, when $\Lambda > 0$, a Minkowski one, when $\Lambda = 0$, and an anti-de Sitter asymptote, when $\Lambda < 0$.

In the full nonminimal theory, there are several characteristic scales. The scales set by q_1, q_2, q_3, the scale set by Λ, the magnetic charge scale Q_m, and the mass scale M. By an imposed choice we reduce the nonminimal parameters from three to two, having thus a five parameter solution, with parameters q, $\bar{q}$ say, Λ, Q_m and M. We have then five scales all of which are important in the modeling of the causal structure of the nonminimally objects that we find, namely, magnetic monopoles and black holes. We show that in our nonminimal model the equation determining the horizon radii can be reduced to an algebraic equation of the sixth order and contains five parameters. Other radii, like those defined by minima, maxima, and inflection are important. For instance, for a positive cosmological constant, there is a critical $\Lambda_c = Q_m^2/972\bar{q}^2$ for which the solution admits a quadruple horizon, the existence of a Λ_c being reminiscent of the $\Lambda_c = 4\pi\rho/3$ for a given energy density ρ that characterizes both the Einstein static and Eddington-Lemaître dynamical universes. Thus, causal structure of these spacetimes is predetermined by the interplay between the characteristic scales. Therefore, we deal now with a new classification task and focus on its complete representation. We apply our classification to the Drummond-Hathrell nonminimal theory that describe nonminimal black holes and to the set of regular black holes previously treated.

The paper is organized as follows. In Sec. II, we revise the elements of the nonminimal Einstein-Yang-Mills theory, the Wu-Yang-type solution for the gauge field and write the nonminimal master equations of the model reduced for a static spherically symmetric spacetime. Sec. III is devoted to constrain the three nonminimal parameters into two to have a five parameter family of exact solutions of the nonminimally Einstein equations. We present the solutions in an explicit form, discuss the role of the nonminimal and the other parameters as well as putting constraining on the whole set of parameters. A preliminary analysis of the equations and horizons is performed. In Secs. IV, V, and VI we present the complete classification of the solutions for $\Lambda > 0$, $\Lambda = 0$ and $\Lambda < 0$, respectively. In Sec. VII, we present a table which summarized the classification of horizons. In Sec. VIII, we discuss an example of the presented classification: we consider the causal structure of the Drummond-Hathrell-type nonminimal theory. In Sec. IX, we mention an example of the presented classification: the nonminimal regular black hole. In Sec. X, we conclude.

II. NONMINIMAL EINSTEIN-YANG-MILLS THEORY: GENERAL FORMALISM AND KEY EQUATIONS FOR STATIC SPHERICALLY SYMMETRIC OBJECTS

We follow the version of the nonminimal Einstein-Yang-Mills theory, which has been formulated in [26] as an $SU(N)$ generalization of the three-parameter nonminimal Einstein-Maxwell theory [20]. We recall its key elements.

A. General formalism and master equations

1. Action functional

The action functional for the nonminimal Einstein-Yang-Mills theory we propose is

$$S_{\rm NMEYM} = \int d^4x\sqrt{-g}\,\left\{\frac{R+2\Lambda}{8\pi} + \frac{1}{2}F^{(a)}_{ik}F^{ik(a)} + \frac{1}{2}\mathcal{R}^{ikmn}F^{(a)}_{ik}F^{(a)}_{mn}\right\}. \quad (1)$$

Here $g=\det(g_{ik})$ is the determinant of a metric tensor g_{ik}, R is the Ricci scalar, and Λ is the cosmological constant. The Einstein constant $\frac{8\pi G}{c^4}$ is reduced to 8π as we use geometrical units, i.e., $G=1$ and $c=1$. Latin indices without parentheses run from 0 to 3. $F^{(a)}_{mn}$ is the Yang-Mills field strength, with the group index being a Latin index with parentheses, e.g., (a), running from 1 to 3. Repeated group indices should be summed with the Kronecker delta. The nonminimal susceptibility tensor $\mathcal{R}^{ikmn}$ is defined as

$$\mathcal{R}^{ikmn} \equiv \frac{q_1}{2}R\,(g^{im}g^{kn}-g^{in}g^{km}) + \frac{q_2}{2}(R^{im}g^{kn}-R^{in}g^{km}+R^{kn}g^{im}-R^{km}g^{in}) + q_3R^{ikmn}, \quad (2)$$

where R^{ik} and R^{ikmn} are the Ricci and Riemann tensors, respectively, and q_1, q_2, q_3 are phenomenological parameters describing the nonminimal coupling of the Yang-Mills fields with gravitation.

2. SU(2)-symmetric Yang-Mills field

We consider the Yang-Mills fields taking values in the Lie algebra of the gauge group $SU(2)$,

$$\mathbf{A}_m = -i\,\mathbf{t}_{(a)}A^{(a)}_m, \quad (3)$$

$$\mathbf{F}_{mn} = -i\,\mathbf{t}_{(a)}F^{(a)}_{mn}. \quad (4)$$

Here $\mathbf{t}_{(a)}$ are the Hermitian traceless generators of the $SU(2)$ group, $A^{(a)}_i$ and $F^{(a)}_{mn}$ are the Yang-Mills field potential and strength, respectively, and the group index (a) runs from 1 to 3. The Yang-Mills fields $F^{(a)}_{mn}$ are connected with the potentials of the gauge field $A^{(a)}_i$ by the formulas

$$\mathbf{F}_{mn} = \nabla_m\mathbf{A}_n - \nabla_n\mathbf{A}_m + [\mathbf{A}_m,\,\mathbf{A}_n]\,,$$
$$F^{(a)}_{mn} = \nabla_mA^{(a)}_n - \nabla_nA^{(a)}_m + f_{(a)(b)(c)}A^{(b)}_mA^{(c)}_n\,. \quad (5)$$

Here ∇_m is a covariant spacetime derivative and the symbols $f_{(a)(b)(c)}\equiv\varepsilon_{(a)(b)(c)}$ denote the real structure constants of the gauge group $SU(2)$.

The variation of the action (1) with respect to the Yang-Mills potential $A^{(a)}_i$ yields

$$\hat{D}_k\mathbf{H}^{ik} \equiv \nabla_k\mathbf{H}^{ik} + \left[\mathbf{A}_k,\mathbf{H}^{ik}\right] = 0\,. \quad (6)$$

The tensor $\mathbf{H}^{ik}=\mathbf{F}^{ik}+\mathcal{R}^{ikmn}\mathbf{F}_{mn}$ is a non-Abelian analog of the excitation tensor, known in electrodynamics. This analogy allows us to consider $\mathcal{R}^{ikmn}$ as a susceptibility tensor. The gauge covariant derivative $\hat{D}_m$ is defined as

$$\hat{D}_m = \nabla_m + [\mathbf{A}_m,\quad]\,. \quad (7)$$

3. Master equations for the gravitational field

Variation of the action functional $S_{\rm NMEYM}$, Eq. (1), with respect to the metric g_{ik} yields

$$R_{ik} - \frac{1}{2}Rg_{ik} = \Lambda g_{ik} + 8\pi T^{\rm eff}_{ik}\,. \quad (8)$$

The effective stress-energy tensor $T^{\rm eff}_{ik}$ can be divided into four parts:

$$T^{\rm eff}_{ik} = T^{YM}_{ik} + q_1T^{I}_{ik} + q_2T^{II}_{ik} + q_3T^{III}_{ik}\,. \quad (9)$$

The first term

$$T^{YM}_{ik} \equiv \frac{1}{4}g_{ik}F^{(a)}_{mn}F^{mn(a)} - F^{(a)}_{in}F_k{}^{n(a)}, \quad (10)$$

is the stress-energy tensor of the pure Yang-Mills field. The definitions of the other three tensors are related to the corresponding coupling constants q_1, q_2, q_3. Thus,

$$T^{I}_{ik} = R\,T^{YM}_{ik} - \frac{1}{2}R_{ik}F^{(a)}_{mn}F^{mn(a)} + \frac{1}{2}\left[\hat{D}_i\hat{D}_k - g_{ik}\hat{D}^l\hat{D}_l\right]\left[F^{(a)}_{mn}F^{mn(a)}\right], \quad (11)$$

$$T^{II}_{ik} = \frac{1}{2}\hat{D}_l\left[\hat{D}_i\left(F^{(a)}_{kn}F^{ln(a)}\right)+\hat{D}_k\left(F^{(a)}_{in}F^{ln(a)}\right)\right] - \frac{1}{2}g_{ik}\left[\hat{D}_m\hat{D}_l\left(F^{mn(a)}F^{l(a)}_{\ n}\right) - R_{lm}F^{mn(a)}F^{l(a)}_{\ n}\right] - F^{ln(a)}\left(R_{il}F^{(a)}_{kn}+R_{kl}F^{(a)}_{in}\right) - R^{mn}F^{(a)}_{im}F^{(a)}_{kn} - \frac{1}{2}\hat{D}^m\hat{D}_m\left(F^{(a)}_{in}F_k{}^{n(a)}\right), \quad (12)$$

$$T^{III}_{ik} = \frac{1}{4} g_{ik} R^{mnls} F^{(a)}_{mn} F^{(a)}_{ls} - \frac{3}{4} F^{ls(a)} \left(F_i{}^{n(a)} R_{knls} + F_k{}^{n(a)} R_{inls} \right) - \frac{1}{2} \hat{D}_m \hat{D}_n \left[F_i{}^{n(a)} F_k{}^{m(a)} + F_k{}^{n(a)} F_i{}^{m(a)} \right] . \quad (13)$$

Now we consider the formulation of the master equations in the context of a static spherically symmetric magnetic spacetime, with a Wu-Yang ansatz.

B. Wu-Yang ansatz and master equations reduced to spherical symmetry

1. Exact Wu-Yang magnetic-type solution to the Yang-Mills equations

The gauge field is considered to be characterized by the Wu-Yang magnetic ansatz (see, e.g., [26–30] and references therein), i.e.,

$$\mathbf{A}_0 = \mathbf{A}_r = 0 \,, \quad \mathbf{A}_\theta = i \mathbf{t}_\varphi, \quad \mathbf{A}_\varphi = -i\nu \sin\theta \, \mathbf{t}_\theta \,. \quad (14)$$

The magnetic parameter ν is a nonvanishing integer. The generators $\mathbf{t}_r$, $\mathbf{t}_\theta$, and $\mathbf{t}_\varphi$ are position-dependent and are connected with the standard generators $\mathbf{t}_{(1)}$, $\mathbf{t}_{(2)}$, and $\mathbf{t}_{(3)}$ of the $SU(2)$ group as follows,

$$\mathbf{t}_r = \cos\nu\varphi \;\; \sin\theta \, \mathbf{t}_{(1)} + \sin\nu\varphi \;\; \sin\theta \, \mathbf{t}_{(2)} + \cos\theta \, \mathbf{t}_{(3)},$$
$$\mathbf{t}_\theta = \partial_\theta \mathbf{t}_r, \qquad \mathbf{t}_\varphi = \frac{1}{\nu \sin\theta} \, \partial_\varphi \mathbf{t}_r \,. \quad (15)$$

They satisfy the following commutation relations

$$[\mathbf{t}_r, \mathbf{t}_\theta] = i \, \mathbf{t}_\varphi \,, \quad [\mathbf{t}_\theta \,, \mathbf{t}_\varphi] = i \, \mathbf{t}_r \,, \quad [\mathbf{t}_\varphi, \mathbf{t}_r] = i \, \mathbf{t}_\theta \,. \quad (16)$$

For this ansatz, the field strength tensor has only one nonvanishing component,

$$\mathbf{F}_{\theta\varphi} = i\nu \sin\theta \, \mathbf{t}_r \,. \quad (17)$$

Clearly, it is a magnetic-type solution and depends essentially on the magnetic parameter ν.

2. Reduced gravity field equations

Let us now consider a static spherically symmetric spacetime with metric given by

$$ds^2 = \sigma^2 N dt^2 - \frac{dr^2}{N} - r^2 \left(d\theta^2 + \sin^2\theta d\varphi^2 \right) \,, \quad (18)$$

where t, r, θ, φ spacetime spherical coordinates. Here σ and N are functions depending on the radial variable r only. Early Einstein-Maxwell models for such a metric with a central electric charge [21–25] and a central magnetic charge [26–28] were studied in the case $\Lambda = 0$. In [29, 30], we eliminated this condition, and, in particular, in [30] we studied regular black holes with Λ positive and negative.

The nonminimal gravity field equations in the spherical symmetric static case have then the form

$$\frac{1-N}{r^2} - \frac{N'}{r} - \Lambda = \frac{\nu^2}{r^4} \left[\frac{1}{2} - q_1 \frac{N'}{r} + (13q_1 + 4q_2 + q_3) \frac{N}{r^2} - \frac{q_1 + q_2 + q_3}{r^2} \right] , \quad (19)$$

$$\frac{1-N}{r^2} - \frac{N'}{r} - \frac{2N\sigma'}{r\sigma} - \Lambda = \frac{\nu^2}{r^4} \left[\frac{1}{2} - q_1 \frac{N'}{r} - 2q_1 \frac{N\sigma'}{r\sigma} - (7q_1 + 4q_2 + q_3) \frac{N}{r^2} - \frac{q_1 + q_2 + q_3}{r^2} \right] , \quad (20)$$

$$\frac{1}{r} N' + N \frac{\sigma'}{r\sigma} + \frac{3\sigma'}{2\sigma} N' + N \frac{\sigma''}{\sigma} + \frac{1}{2} N'' + \Lambda = \frac{\nu^2}{r^4} \left[\frac{1}{2} - \frac{3q_1 \sigma' N'}{2\sigma} - \frac{q_1 N \sigma''}{\sigma} - \frac{q_1 N''}{2} - (7q_1 + 4q_2 + q_3) \left(\frac{(\sigma N)'}{\sigma r} - \frac{2N}{r^2} \right) + (q_1 + q_2 + q_3) \frac{2}{r^2} \right] . \quad (21)$$

A prime denotes a derivative with respect to the radial variable r. As usual, the compatibility conditions related to the Bianchi identities are satisfied.

III. EXACT SOLUTIONS TO THE GRAVITY FIELD EQUATIONS: FIVE -PARAMETER FAMILY OF EXACT SOLUTIONS AND GENERIC ANALYSIS

A. Five-parameter family of exact solutions

1. General equations

In spherical symmetry, Eq. (21) is a consequence of Eqs. (19) and (20). The difference between Eq. (19) and Eq. (20) gives an equation for the function $\sigma(r)$ alone, which does not depend on Λ, namely,

$$\frac{\sigma'}{\sigma} \left(1 - \frac{2Q_m^2 q_1}{r^4} \right) = \frac{2Q_m^2 (10q_1 + 4q_2 + q_3)}{r^5} \,. \quad (22)$$

Then, Eq. (20) gives the key equation for the metric function $N(r)$,

$$rN' \left(1 - \frac{2Q_m^2 q_1}{r^4} \right) + N \left[1 + \frac{2Q_m^2}{r^4} (13q_1 + 4q_2 + q_3) \right] = 1 - \frac{Q_m^2}{r^2} + \frac{2Q_m^2}{r^4} (q_1 + q_2 + q_3) - \Lambda r^2 \,. \quad (23)$$

In Eqs. (22) and (23),

$$Q_m^2 = 4\pi\nu^2 \,, \quad (24)$$

defining Q_m as the magnetic charge of the solution.

2. The trivial solution

The trivial solution in this context is when q_1, q_2, and q_3 vanish,

$$q_1 = q_2 = q_3 = 0\,, \tag{25}$$

Then in this limit, Eqs. (22)-(23), admit the solution $\sigma(r) = 1$, and Eq. (23) yields the Reissner-Nordström solution with a cosmological constant, i.e.,

$$\sigma(r) = 1\,, \tag{26}$$

$$N = 1 - \frac{2M}{r} + \frac{Q_m^2}{r^2} - \frac{1}{3}\Lambda r^2\,. \tag{27}$$

It is the minimally coupled magnetic Reissner-Nordström solution with a cosmological constant.

3. Solution for $q_1 = 0$

When $q_1 = 0$, Eqs. (22)-(23) with the asymptotic condition $\sigma(r \to \infty) \to 1$ yield

$$\sigma(r) = \exp\left(-\frac{Q_m^2(4q_2 + q_3)}{2r^4}\right)\,, \tag{28}$$

$$\begin{aligned} N(r) = 1 - \frac{\Lambda r^2}{3} - \frac{1}{r}\,\exp\left(\frac{Q_m^2(4q_2+q_3)}{2r^4}\right) \\ \times\left\{2M - Q_m^2\int_r^{+\infty}\frac{dx}{x^2}\left[1 - \frac{2\Lambda}{3}(4q_2+q_3)\right.\right. \\ \left.\left. + \frac{6q_2}{x^2}\right]\exp\left(-\frac{Q_m^2(4q_2+q_3)}{2x^4}\right)\right\}. \end{aligned} \tag{29}$$

In particular, if $4q_2 + q_3 = 0$, we have a solution with one independent nonminimal parameter, q_2 say, and so an overall four parameter solution, given by

$$\sigma(r) = 1, \tag{30}$$

$$N(r) = 1 - \frac{2M}{r} + \frac{Q_m^2}{r^2} + \frac{2Q_m^2 q_2}{r^4} - \Lambda r^2. \tag{31}$$

This solution has an interest of its own, for instance, it has a more complex causal structure than the Reissner-Nordström solution. But here we want to discuss the more general case when $q_1 \neq 0$ giving a solution which in general has two independent nonminimal parameters, and so it is a five parameter solution

4. General solution

To find the general solution we define ξ as

$$\xi \equiv \frac{10q_1 + 4q_2 + q_3}{4q_1}\,. \tag{32}$$

Then, for generic q_1, q_2, q_3, Eq. (22) together with the asymptotic condition $\sigma(r \to \infty) \to 1$ yields

$$\sigma(r) = \left(1 - \frac{2Q_m^2 q_1}{r^4}\right)^{\xi}\,. \tag{33}$$

The cases $q_1 = q_2 = q_3 = 0$, and $q_1 = 0$ and $4q_2 + q_3 = 0$ are particular cases of Eq. (22) which we have mentioned. Eq. (23) together with the asymptotic condition $N(r \to \infty) \to 1 - \Lambda r^2/3$ yields

$$\begin{aligned} N = 1 - \frac{\Lambda r^2}{3} - \frac{1}{r}\left(1 - \frac{2Q_m^2 q_1}{r^4}\right)^{-(\xi+1)} \\ \times\left\{2M - \int_r^{+\infty}\frac{dx}{x^2}\left[Q_m^2\left[1 - \frac{2\Lambda}{3}(11q_1 + 4q_2 + q_3)\right]\right.\right. \\ \left.\left. + \frac{6Q_m^2}{x^2}(4q_1 + q_2)\right]\left(1 - \frac{2Q_m^2 q_1}{x^4}\right)^{\xi}\right\}, \end{aligned} \tag{34}$$

The general setup provided by Eqs. (32)-(34) yields, so far, a six-parameter family of exact solutions: the three nonminimal parameters q_1, q_2, and q_3, the cosmological constant Λ, the magnetic charge Q_m of the Wu-Yang gauge field, and the mass M of the solution.

5. General analysis

Equations (32)-(34) yield a six-parameter family of exact solutions. The parameters are the three nonminimal parameters q_1, q_2, and q_3, the cosmological constant Λ, the magnetic charge parameter Q_m, and the asymptotic mass M. We now choose one appropriate relation between the three nonminimal parameters q_1, q_2, and q_3 and reduce the family to a five-parameter family of exact solutions. For that we have to discuss the parameter ξ given in Eq. (32). To find constraints on the parameter ξ, and so, on q_1, q_2, and q_3, we study the behavior of the functions at some finite r, $r \to \infty$, and $r \to 0$.

For some finite r, we find that we should put $q_1 \leq 0$. This is because for some finite r, when $q_1 > 0$ nasty singularities appear in $\sigma(r)$ and $N(r)$ in Eqs. (33)-(34). The case $q_1 = 0$ was treated before and it has curvature singularities at $r = 0$. Thus we put

$$q_1 < 0\,. \tag{35}$$

When $r \to \infty$, these solutions, Eqs. (33)-(34), asymptotically behave as

$$\sigma = 1 + \frac{2Q_m^2 q_1}{r^4}\,\xi + \dots\,, \tag{36}$$

$$\begin{aligned} N = -\frac{\Lambda r^2}{3} + 1 - \frac{2M}{r} \\ + \frac{Q_m^2}{r^2}\left[1 - \frac{2\Lambda}{3}(11q_1 + 4q_2 + q_3)\right] \\ + \frac{2Q_m^2}{r^4}\,(4q_1 + q_2) + \dots\,. \end{aligned} \tag{37}$$

Thus, $\sigma(\infty) = 1$ for arbitrary ξ. As for $N(r \to \infty)$, it displays a dS asymptotic behavior when Λ is positive, a Minkowski asymptotic behavior when $\Lambda = 0$, and an AdS behavior when Λ is negative. Thus, there are no constraints on the parameter ξ in the limit $r \to \infty$.

When $r \to 0$ the analysis is subtle. It should be divided into two cases, $\xi < -3/4$ and $\xi \geq -3/4$.
$\xi < -3/4$: When $\xi \leq -3/4$ and $q_1 < 0$, we have $\sigma(0) = 0$ and $N(0) = \infty$; when $q_1 = 0$ and $4q_2 + q_3 > 0$, the metric functions have the same behavior at the origin; if $q_1 = 0$ and $4q_2 + q_3 < 0$, $\sigma(0) = \infty$ and $N(0)$ is finite. Finally, if $q_1 = 0$, $4q_2 + q_3 = 0$, but $q_2 \neq 0$, we have $\sigma(0) = 1$ and $N(0) = \infty$. From the point of view of invariants divergency, all these cases blow up at the origin faster than $1/r^4$.
$\xi \geq -3/4$: When $\xi \geq -3/4$ and $q_1 = 0$ curvature singularities appear at the origin. On the other hand, when $\xi \geq -3/4$ and $q_1 < 0$, the Ricci scalar square, the Ricci tensor square scalar, and the Kretschmann scalar are given as $r \to 0$ by,

$$R^2 = \frac{4}{r^4}\left[4\xi N(0)(4\xi - 1) + N(0) - 1\right]^2 . \tag{38}$$

$$R_{ik}R^{ik} = \tfrac{2}{r^4}\left[32\xi^2 N(0)^2(8\xi^2+1) - 8\xi N(0)(N(0)-1) + (N(0)-1)^2\right] , \tag{39}$$

$$R_{ikmn}R^{ikmn} = \tfrac{4}{r^4}\left[16\xi^2 N(0)^2(16\xi^2+8\xi+3) + (N(0)-1)^2\right] , \tag{40}$$

respectively, and where $N(0)$ is $N(r)$ at $r = 0$, i.e.,

$$N(0) = 1 - \frac{3(4q_1 + q_2)}{q_1(4\xi + 3)} = \frac{q_1 + q_2 + q_3}{13q_1 + 4q_2 + q_3} . \tag{41}$$

So all quadratic curvature invariants behave at $r \to 0$ according to the formula

$$\mathrm{Inv(r \to 0)} = \frac{C}{r^4} , \tag{42}$$

for some constant C that can be extracted from Eqs. (38)-(41). We find that $C \geq 0$. The case $C = 0$ happens when $N(0) = 1$ and $\xi = 0$. In this case, all invariants are zero at the center everywhere and the corresponding solutions yield regular objects and regular black holes. This case has been treated in [30]. Although important this case is too particularized. In order to pick up a more general and also interesting case for $\xi > -3/4$ and $q_1 < 0$, we have to address the behavior of the functions $\sigma(r)$ and $N(r)$. (a) The case $N(0)$ finite (and not equal to 1) and $\xi = 0$ stands out clearly. In this case, $\sigma(0) = 1$, $g_{00}(0) = N(0)$ is finite and $g_{rr}(0) = 1/N(0)$ is also finite. Thus, the singularities that appear at $r = 0$ are of the conical type and so are milder singularities. To be complete let us list the other cases: (b) when $N(0) = 1$ and $-3/4 < \xi < 0$, then $\sigma(0) = 0$, $g_{00}(0) = 0$, $g_{rr}(0) \neq \infty$; (c) when $N(0) \neq 1$, $N(0) \neq 0$, but $-3/4 < \xi < 0$, here $\sigma(0) = 0$ and $g_{00}(0) = 0$, $g_{rr}(0) \neq \infty$; (d) when $N(0) = 0$, and $-3/4 < \xi < 0$, here $\sigma(0) = 0$ and $g_{00}(0) = 0$, $g_{rr}(0) = \infty$. We opt for studying case (a) in detail.

So, below we consider models with $\xi = 0$, or $10q_1 + 4q_2 + q_3 = 0$, and $q_1 < 0$ only, thus reducing the six-parameter family of solutions to a five-parameter one. This five-parameter family of solutions has many particular cases. The trivial case $q_1 = q_2 = q_3 = 0$, and the case $q_1 = 0$ and q_2 and q_3 free have already been treated and will not take part in the following analysis. The case $10q_1 + 4q_2 + q_3 = 0$ and $4q_1 + q_2 = 0$ is the regular black hole case already mention and studied in detail in [30]. And, of course, there are other examples as we will see below.

So let us consider explicitly the condition $\xi = 0$, i.e.,

$$10q_1 + 4q_2 + q_3 = 0 , \tag{43}$$

which guarantees that $\sigma(r) = 1$. We define q and $\bar{q}$ such that

$$q \equiv -q_1 , \tag{44}$$

$$\bar{q} \equiv q_2 + 3q_1 , \tag{45}$$

so that from Eq. (43), we find

$$-2q - 4\bar{q} = q_3 . \tag{46}$$

Due to Eq. (43), we have now two nonminimal parameters, q and $\bar{q}$, instead of the initial three. From Eq. (35), assume $q > 0$, so that there are no wild singularities at finite r.

6. *Explicit five-parameter family of solutions with two nonminimal parameters q and $\bar{q}$, Λ, Q_m, and M*

We thus deal with a five-parameter family of solutions, q, $\bar{q}$, Λ, Q_m, and M, instead of six. The metric functions $\sigma(r)$ and $N(r)$ take then the following explicit form

$$\sigma(r) \equiv 1 , \tag{47}$$

$$N = 1 - \frac{\Lambda r^2}{3} + \frac{r^2 Q_m^2\left(1 + \frac{2\Lambda q}{3}\right) - 2Mr^3 + 2Q_m^2(\bar{q} - q)}{r^4 + 2Q_m^2 q} , \tag{48}$$

When $q > 0$, this function is finite for all finite values of r, and the value $N(0)$ is equal now to $N(0) = \frac{\bar{q}}{q}$. The first derivative takes zero value at the center, $N'(0) = 0$. The second derivative at the center $N''(0) = \frac{1}{q}$ depends on the nonminimal coupling parameter q only, and is positive for $q > 0$. This means that $r = 0$ is the minimum of the regular function $N(r)$, which near the center has the form

$$N(r) = \frac{\bar{q}}{q} + \frac{1}{2q}r^2 + \dots . \tag{49}$$

In addition to the root $r = 0$, the equation $N'(r)$=0 can have other root $r = r_{\min} > 0$ related to a minimum of the function $N(r)$. Clearly, at this radius any massive particle can be in a stable equilibrium. This point is a finite r equilibrium point in contrast to the central equilibrium point $r = 0$.

7. *Roles and constraints on the five parameters q and $\bar{q}$, Λ, Q_m, and M*

We now discuss the roles and constraints on the five parameters q, $\bar{q}$, Λ, Q_m, and M. As we have pointed out the parameter q must obey

$$q > 0\,, \tag{50}$$

such that there are no singularities at some finite r. The parameter $\bar{q}$ should obey

$$-\infty < \bar{q} < \infty\,, \tag{51}$$

i.e., it is not restricted.

The main role of the parameter Λ is at infinity. At $r = 0$ the cosmological term Λr^2 vanishes. At infinity one has a spacetime asymptotically dS for

$$\Lambda > 0\,, \tag{52}$$

asymptotically Minkowski for

$$\Lambda = 0\,, \tag{53}$$

and asymptotically AdS for $\Lambda < 0$. From Eq. (48), we see that in order to have a solution with $Q^2_{\text{eff}\,m} \equiv Q^2_m\left(1 + \frac{2\Lambda q}{3}\right) \geq 0$, we must impose

$$-\frac{3}{2q} \leq \Lambda < 0\,. \tag{54}$$

The parameter $Q^2_m \equiv 4\pi\nu^2$ is the magnetic charge of the Wu-Yang field. Not wanting to consider imaginary Wu-Yang magnetic charge ν we discuss solutions for which

$$Q^2_m > 0\,. \tag{55}$$

Moreover, the redefined nonminimal coupling constants q and $\bar{q}$ enter the solutions given in Eq. (48) in the form of a product with Q^2_m. This means that the case $Q_m = 0$ does not yield nonminimal solutions. In addition, one sees that indeed the product $(Q^2_m q)^{\frac{1}{4}}$ plays the role of an effective nonminimal scale (see, Eq. (48)), and the value of $(Q^2_m q)^{\frac{1}{4}}$ predetermines the number and type of horizons.

The parameter M is the asymptotic mass. In order to have the usual solutions with positive mass at infinity, we impose

$$M > 0\,. \tag{56}$$

B. Horizon classification: Auxiliary function and preliminary analysis

When Eq. (48) obeys

$$N(r_h) = 0\,, \tag{57}$$

and the roots r_h are real and positive, we are in the presence of horizons at those radii. Since the equation $N(r_h) = 0$ can be reduced to an algebraic equation of order six, the number of horizons is not more than six. We show that, in fact, the number of horizons cannot be more than four.

The horizon number is of major importance in the study of any spacetime causal structure. In this structure it is also important to classify the horizons and visualize them in figures. In order to classify the solutions with a different number of horizons, we used here a method applied earlier [27] (see also [30]). This method is based on the introduction of an auxiliary function $f(r)$ in the following context. The equation $N(r) = 0$ with $N(r)$ given in Eq. (48) can be rewritten in the form

$$2M = f(r)\,, \tag{58}$$

$$f(r) \equiv -\frac{\Lambda r^3}{3} + r + \frac{Q^2_m}{r} + \frac{2Q^2_m\bar{q}}{r^3}\,. \tag{59}$$

To count the horizon number we have to determine the number of points in which the plot of the function $y = f(r)$ is crossed by the horizontal mass line $y = 2M$. From a physical point of view, this procedure shows how many horizons there are, when the mass of the object is equal to M. Clearly, the parameter $\bar{q}$ regulates the behavior of $f(r)$ at $r \to 0$, and the parameter Λ predetermines the behavior of $f(r)$ at $r \to \infty$. Thus, these two parameters are the principal parameters in this analysis. Below we describe the details of the corresponding classification.

To proceed we have to analyze the equation $f'(r) = 0$ which gives the extrema of the function $f(r)$. The equation $f'(r) = 0$ can be rewritten as the bicubic equation

$$\Lambda r^6 - r^4 + Q^2_m r^2 + 6Q^2_m\bar{q} = 0\,. \tag{60}$$

We also have to analyze the important equation $f''(r) = 0$ which can also be rewritten as the following bicubic equation

$$-\Lambda r^6 + Q^2_m r^2 + 12Q^2_m\bar{q} = 0\,. \tag{61}$$

First we analyze the $f'(r) = 0$ equation. Considering then the bicubic equation, Eq. (60), in terms of the auxiliary quantity,

$$X \equiv r^2 - \frac{1}{3\Lambda}\,, \tag{62}$$

one gets a cubic equation of the form

$$X^3 + LX + M = 0\,. \tag{63}$$

The corresponding discriminant $D = -(4L^3 + 27M^2)$ is now of the form,

$$D = -\frac{3Q_m^4}{2\Lambda^4}\left\{\left(1+18\Lambda\bar{q}+\frac{Q_m^2}{27\bar{q}}\right)^2 - \left[\left(1+\frac{2Q_m^2}{54\bar{q}}\right)^2+\frac{1}{3}+8\frac{\bar{q}}{Q_m^2}\right]\right\}. \quad (64)$$

Equation (63) gives three roots X_1, X_2, X_3, with properties

$$X_1X_2X_3 = -\frac{6Q_m^2\bar{q}}{\Lambda}, \quad X_1+X_2+X_3 = \frac{1}{\Lambda}. \quad (65)$$

Clearly, when $\bar{q}$ is negative and Λ is positive, it is admissible that all three roots are positive, thus, three is the maximal number of extrema. When $D = 0$, we deal with a special value of the parameter, $\Lambda_{\rm special}$, given by

$$\Lambda_{\rm special} = \frac{1}{18\bar{q}}\left[-\left(1+\frac{Q_m^2}{27\bar{q}}\right) \pm \sqrt{\left(1+\frac{Q_m^2}{18\bar{q}}\right)^3\frac{8\bar{q}}{Q_m^2}}\right]. \quad (66)$$

When $\bar{q} \geq -\frac{Q_m^2}{18}$, $\Lambda_{\rm special}$ is real. When $\bar{q} = -\frac{Q_m^2}{18}$, we have that $\Lambda_{\rm special} = \frac{1}{3Q_m^2}$, which is positive.

We also have to analyze the important equation $f''(r) = 0$, i.e., Eq. (61). This equation gives the inflexion points of the function $f(r)$. The analysis on the number of inflexion points, provided by Eq. (61) is a convenient tool for the required classification. The analysis of extrema, derived from Eq. (60), is a supplementary tool describing some details of the classification. In terms of the auxiliary variable,

$$Y \equiv r^2, \quad (67)$$

Eq. (61) gives a cubic equation of the type

$$Y^3 + PY + Q = 0, \quad (68)$$

for which the discriminant is $\Delta \equiv -(4P^3 + 27Q^2)$, i.e.,

$$\Delta = \frac{Q_m^6}{\Lambda^2}\left(\frac{1}{\Lambda} - \frac{972}{Q_m^2}\bar{q}^2\right). \quad (69)$$

The product and the sum of the roots of Eq. (68) are, respectively,

$$Y_1Y_2Y_3 = \frac{12Q_m^2\bar{q}}{\Lambda}, \quad Y_1+Y_2+Y_3 = 0. \quad (70)$$

Since the sum of roots is equal to zero, at least one real root is negative or the real part of complex conjugated pair of roots is negative. Thus, two is the maximal number of inflexion points. Since the sign of the product $Y_1Y_2Y_3$ of the roots depends on the ratio of the parameters $\bar{q}$, Λ, and Q_m^2, (see Eq. (70)), for the $\Lambda > 0$ case, below we distinguish eight different situations using the critical value of the cosmological constant Λ_c, for which the discriminant Δ vanishes, i.e.,

$$\Lambda_c = \frac{Q_m^2}{972\,\bar{q}^2}. \quad (71)$$

So, clearly, $\Lambda_c > 0$. The existence of a Λ_c is reminiscent of the $\Lambda_c = 4\pi\rho/3$ for a given energy density ρ that characterizes both the Einstein static and Eddington-Lemaître dynamical universes.

According to these preliminary considerations, the classification of horizons can be based on the analysis of the Eqs. (58)-(59) with respect to the parameters $\bar{q}$ and Λ. Below, we fix the cosmological constant according to $\Lambda > 0$, $\Lambda = 0$, and $\Lambda < 0$, and vary the parameter $\bar{q}$.

IV. EXACT SOLUTIONS WITH A POSITIVE COSMOLOGICAL CONSTANT, $\Lambda > 0$

The case $\Lambda > 0$ is subdivided into $\bar{q} < 0$ and $\bar{q} \geq 0$. Moreover, when the cosmological constant is positive, $\Lambda > 0$, the discriminant Δ in Eq. (69) can be positive, vanishing, or negative. This means that there is a critical value of the cosmological constant Λ_c which we have found previously, see Eq. (71), given by $\Lambda_c = \frac{Q_m^2}{972\,\bar{q}^2}$, with $\Lambda_c > 0$. So, in the analysis of the case $\Lambda > 0$ we have to distinguish the cases $0 < \Lambda < \Lambda_c$, $\Lambda = \Lambda_c$ and $\Lambda > \Lambda_c$. All panels and plots for this $\Lambda > 0$ case are shown in Fig. 1.

A. The case $\bar{q} < 0$ and $\Lambda > 0$

Here, Eqs. (59), (60), and (61) yield

$$f(r) = -\frac{|\Lambda|r^3}{3} + r + \frac{Q_m^2}{r} - \frac{2Q_m^2|\bar{q}|}{r^3}, \quad (72)$$

$$|\Lambda|r^6 - r^4 + Q_m^2r^2 - 6Q_m^2|\bar{q}| = 0, \quad (73)$$

$$-|\Lambda|r^6 + Q_m^2r^2 - 12Q_m^2|\bar{q}| = 0, \quad (74)$$

respectively. The analysis proceeds as in the previous section.

(1) $0 < \Lambda < \Lambda_c$

In this case, the discriminant given by Eq. (69) is positive, there are three real different roots Y_1, Y_2 and Y_3, and two of them are positive (see Eq. (70)). These two positive real roots r_{i1} and r_{i2} of Eq. (74), are such that $r_{i1} \neq r_{i2}$, i.e., there are two noncoinciding inflexion points of the function $f(r)$. As for the roots X_1, X_2, X_3 of Eq. (73) (see Eq. (65) for the analysis of their signs) one finds that there are three possibilities: there is the possibility of three different real positive roots, the possibility of one real positive root, and the possibility of three real positive roots two of which coincide. The case when three real roots coincide does not give two inflexion points, it is a

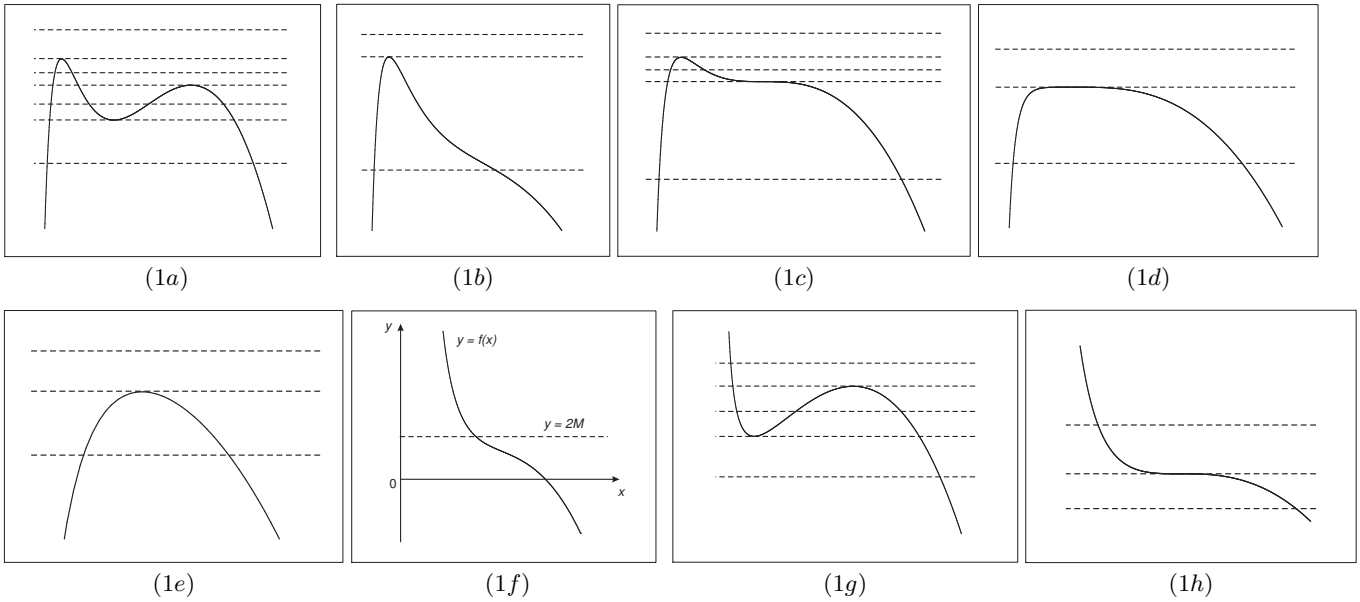

(1a) (1b) (1c) (1d)

(1e) (1f) (1g) (1h)

FIG. 1: $\Lambda > 0$. Sketches of the auxiliary function $f(r) = -\frac{1}{3}\Lambda r^3 + r + Q_m^2 r^{-1} + 2Q_m^2 \bar{q} r^{-3}$ for positive cosmological constant $\Lambda > 0$. At the points r_h, in which the horizontal mass line $y = 2M$ crosses the curve of the function $y = f(r)$, the metric function $N(r)$ takes zero values, i.e., the spheres $r = r_h$ are horizons. Panels (1a), (1b), (1c) (1d), and (1e) show typical cases for which $\bar{q} < 0$, and panels (1f), (1g), and (1h) illustrate the cases for $\bar{q} \geq 0$. In panel (1a) the plot of the function $f(r)$ displays two inflexion points and three extrema. Depending on the mass M, and thus on the mass line $y = 2M$, one can find, counting the intersections from top to bottom, zero, one, two, three, four, three, and two cross-points with $y = f(r)$, respectively. So the spacetime can contain the following number of horizons: zero, one double, two simple, two simple plus one double (corresponding to a maximum), four simple, one simple plus one double (corresponding to a minimum) plus one simple, and two simple one of them being a distant one, horizons. In the case when the heights of the two maxima are equal one gets two double horizons. Also, it is possible that the left maximum of the auxiliary function is lower that the right maximum. The number of horizons remains the same and we find that there is no need to display this curve. Panel (1b) illustrates the solutions with two inflexion points and one maximum. The corresponding number of horizons can be zero, one double, and two simple horizons. Panel (1c) shows solutions for which the second inflexion point coincides with one minimum and one maximum. This case admits zero, one double, two simple, one simple plus one triple, and two simple one of them is a distant one, horizons. Panel (1d) corresponds to the situation, when all inflexion and extremal points coincide, i.e., two maxima coincide with a minimum and two inflexion points. This case admits zero, one quadruple, and two simple horizons one of them is a distant one. Panel (1e) illustrates the case, when there are no inflexion points and there is only one extremum, a maximum. In this case there are zero, one double, and two simples horizons, one of them is a distant one. Panel (1f) depicts the case where one has an inflexion point and there are no extrema. In this case there is only one simple horizon. Panel (1g) corresponds to the situation where there is one inflexion point and a pair of extrema, a minimum comes first, and a maximum comes second. Depending on the mass M one can obtain one, one plus a double one, three simple, a double one plus one distant simple horizon, and one distant simple horizon. Panel (1h) illustrates the case, when the minimum, the inflexion point, and the maximum coincide. Here the possibilities are: one simple horizon, a triple horizon, and one distant simple horizon.

degenerated case. As for the function $f(r)$ itself we find that $f(0) = -\infty$ and $f(\infty) = -\infty$. Thus, taking into account altogether there are three main situations.

The first situation is described in panel (1a) of Fig. 1. The function has one local minimum, two local maxima, and two inflexion points between the corresponding maxima and minimum. The horizontal mass line can cross this plot zero, one, two, three and four times. This means, that this model can admit zero, one double, two simple, two simple plus one double (corresponding to a maximum), and four simple horizons. In the case when the heights of the two maxima are equal one gets two double horizons. There is also a situation where two simple plus one double (corresponding to a minimum) horizon exist, and a different situation where there are two simple horizons, one of them is a distant one.

The second situation is described in panel (1b) of Fig. 1, it has only local maximum. Thus, this model admits zero, one double, and two simple horizons.

The third situation is described in panel (1c) of Fig. 1, it is characterized by the coincidence of the minimum with one maximum and one inflexion point. This case admits zero, one double, two simple, and two horizons, one is simple and the other is triple. There is also a different situation where two simple horizons exist, one of them is a distant one.

Thus, in the case $\bar{q} < 0$ and $0 < \Lambda < \Lambda_c$ we obtain models with zero, one, two, three, or four horizons.

(2) $\Lambda = \Lambda_c$

When the discriminant given by Eq. (69) vanishes, Eq. (74) takes the simple multiplicative form $(r^2 - 18|\bar{q}|)^2(r^2 + 36|\bar{q}|) = 0$. Clearly, for negative $\bar{q}$ there are two coinciding real positive roots of this equation, $r_i = 3\sqrt{2|\bar{q}|}$, and thus, there is one double inflexion point for the function $f(r)$. If, in addition, $|\bar{q}| = Q_m^2/18$, i.e., $\bar{q} = -Q_m^2/18$, Eq. (73) converts into $(r^2 - Q_m^2)^3 = 0$, and thus, two maxima coincide with the minimum at $r = |Q_m|$ and coincides with double inflexion point $r_i = 3\sqrt{2|\bar{q}|}$. We also have $f(0) = -\infty$ and $f(\infty) = -\infty$. The sketch of the corresponding function $f(r)$ is represented in panel $(1d)$ of the Fig. 1. It can be considered as a limiting case of panel $(1b)$. This case admits zero, one quadruple, and two simple horizons, one of them is a distant one.

(3) $\Lambda > \Lambda_c$

When the discriminant given by Eq. (69) is negative, there is one real root Y_1, and it is negative. So, there are no real positive roots and no inflexion points of the function $f(r)$. Again $f(0) = -\infty$ and $f(\infty) = -\infty$. There is only one variant with one extremum, a maximum of the function $f(r)$. See panel $(1e)$ of Fig. 1. In this case there are zero, one double, and two simples horizons, one of them is a distant one.

B. The case $\bar{q} \geq 0$ and $\Lambda > 0$

For $\bar{q} = 0$, Eqs. (59), (60), and (61) are given by

$$f(r) = -\frac{|\Lambda| r^3}{3} + r + \frac{Q_m^2}{r}\,, \tag{75}$$

$$|\Lambda| r^6 - r^4 + Q_m^2 r^2 = 0\,, \tag{76}$$

$$-|\Lambda| r^6 + Q_m^2 r^2 = 0\,, \tag{77}$$

respectively.

One has one inflexion point $r_i = \left(\frac{Q_m^2}{|\Lambda|}\right)^{\frac{1}{4}}$, there are at most two extrema at $r_{\rm extr1} = \sqrt{\frac{1}{2|\Lambda|}\left(1 + \sqrt{1 - 4Q_m^2|\Lambda|}\right)}$ and $r_{\rm extr2} = \sqrt{\frac{1}{2|\Lambda|}\left(1 - \sqrt{1 - 4Q_m^2|\Lambda|}\right)}$, and at $4Q_m^2|\Lambda| = 1$ the extrema coincide with the inflexion point. Also, $f(0) = +\infty$, $f(\infty) = -\infty$. For $\bar{q} = 0$, at $r = 0$ one has a horizon that is singular. Apart from this initial analysis $\bar{q} = 0$ and $\bar{q} > 0$ have the same type of behavior.

We analyze it in the following for a generic $\bar{q} > 0$. Here, Eqs. (59), (60), and (61) yield

$$f(r) = -\frac{|\Lambda| r^3}{3} + r + \frac{Q_m^2}{r} + \frac{2Q_m^2|\bar{q}|}{r^3}\,, \tag{78}$$

$$|\Lambda| r^6 - r^4 + Q_m^2 r^2 + 6Q_m^2|\bar{q}| = 0\,, \tag{79}$$

$$-|\Lambda| r^6 + Q_m^2 r^2 + 12Q_m^2|\bar{q}| = 0\,, \tag{80}$$

respectively.

(1) $0 < \Lambda < \Lambda_c$

Here the discriminant given in Eq. (69) is positive and there are three real roots Y_1, Y_2 and Y_3. Since the product of the roots is positive and the sum is equal to zero, two of them should be negative and one positive. This means that there exists only one positive real value r_i, the root of Eq. (80), indicating one inflexion point of the function $f(r)$. The product of the roots X_1, X_2, X_3 is negative and their sum is positive. Thus, one has two possibilities: first, there is a pair of complex conjugated roots and one negative real root, and second, there are two positive and one negative real roots. The case with three negative real roots should be excluded. Taking into account that in this case $f(0) = +\infty$ and $f(\infty) = -\infty$, we see that there are three possible situations.

The first situation is described in panel $(1f)$ of Fig. 1. There is one inflexion point but there are no extrema. The mass line crosses the curve only once, and this means that inevitably there is one and only one simple horizon.

The second situation is described in panel $(1g)$ of Fig. 1. The curve $f(r)$ has one local minimum, one local maximum and one inflexion point between them. Depending on the mass M one can obtain one, one plus a double one, three simple, a double one plus one distant simple horizon, and one distant simple horizon.

The third situation is described in panel $(1h)$ of Fig. 1. This case is degenerated, i.e., the maximum, the minimum and the inflexion points coincide. One can have one simple horizon, a triple horizon, and one distant simple horizon.

Thus, in the case $\bar{q} > 0$ and $0 < \Lambda < \Lambda_c$ we obtain models with at least one horizon, and two or three horizons can appear for specific values of the mass M.

(2) $\Lambda = \Lambda_c$

The discriminant in Eq. (69) vanishes. There are three real roots: one positive and two coinciding negative roots. Thus, there is one real positive root r_{1i}, and so one inflexion point of the function $f(r)$. Since $f(0) = +\infty$ and $f(\infty) = -\infty$, the plots of this function $f(r)$ are given in panels $(1f)$, $(1g)$ and $(1h)$ of Fig. 1.

(3) $\Lambda > \Lambda_c$

The discriminant in Eq. (69) is negative. There is one real positive root, say, Y_1, so one positive real root r_{1i}, and thus one inflexion point of the function $f(r)$. Since $f(0) = +\infty$ and $f(\infty) = -\infty$, we deal with one of the situations described in panels $(1f)$, $(1g)$, and $(1h)$ of Fig. 1.

V. EXACT SOLUTIONS WITH ZERO COSMOLOGICAL CONSTANT, $\Lambda = 0$

The case $\Lambda = 0$ is subdivided into $\bar{q} < 0$ and $\bar{q} \geq 0$. All panels and plots for this $\Lambda = 0$ case are shown in Fig. 2.

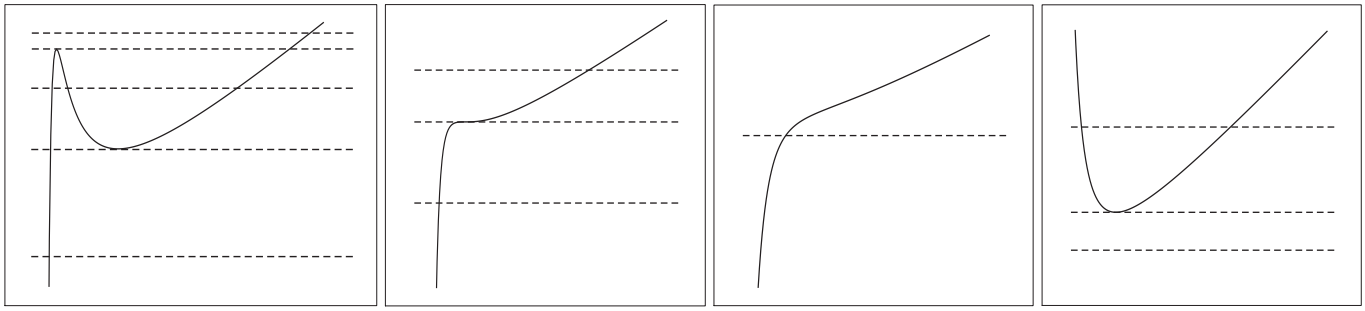

(2a) (2b) (2c) (2d)

FIG. 2: $\Lambda = 0$. Sketches of the auxiliary function $f(r) = r + Q_m^2 r^{-1} + 2Q_m^2 \bar{q} r^{-3}$ for zero cosmological constant $\Lambda = 0$. At the points r_h, in which the horizontal mass line $y = 2M$ crosses the curve of the function $y = f(r)$, the metric function $N(r)$ takes zero values, i.e., the spheres $r = r_h$ are horizons. The plots on panels (2a), (2b), (2c) show typical cases for which $\bar{q} < 0$, and panel (2d) illustrates the cases for $\bar{q} \geq 0$. In panel (2a) the plot of the function $f(r)$ displays one inflexion point and two extrema. Depending on the mass M, and thus on the mass line $y = 2M$, one can find one, one double plus one simple, three simple, one simple plus one double, and one simple horizon. In the case the extrema coincide one has a quadruple horizon, not shown in panel. In panel (2b) the inflexion point coincides with an extremum. One can find one simple horizon. In panel (2c) there is one inflexion point and no extrema. One can find one simple horizon. In panel (2d) there are no inflexion points and there is one extremum, a minimum. In this case there are zero, one double, and two simple horizons.

A. The case $\bar{q} < 0$ and $\Lambda = 0$

Here, Eqs. (59), (60), and (61) yield

$$f(r) = r + \frac{Q_m^2}{r} - \frac{2Q_m^2}{r^3}|\bar{q}|\,, \tag{81}$$

$$r^4 - Q_m^2 r^2 + 6Q_m^2|\bar{q}| = 0\,, \tag{82}$$

$$r^2 = 12|\bar{q}|\,, \tag{83}$$

respectively. Clearly, the case $\Lambda = 0$ is much simpler for classification than $\Lambda > 0$, since Eq. (83) is now a quadratic equation (instead of bicubic) for obtaining the inflexion point, and Eq. (82) is a biquadratic equation for obtaining of extrema, instead of the corresponding bicubic equation. The auxiliary function $f(r)$, Eq. (81), has the following asymptotic properties: $f(0)=-\infty$, $f(\infty)=\infty$. There is one inflexion point at $r=\sqrt{12|\bar{q}|}$. The parameter $\frac{24\bar{q}}{Q_m^2}$ is now the critical parameter of the model, and we have three intrinsic situations.

The first situation is displayed on panel (2a) of Fig. 2 and corresponds to the case when $\frac{24\bar{q}}{Q_m^2} < 1$. There are two extrema: the maximum at $r_{\rm extr1}=\sqrt{\frac{Q_m^2}{2} - \sqrt{\frac{Q_m^4}{4} - 6Q_m^2|\bar{q}|}}$, and minimum at $r_{\rm extr2}=\sqrt{\frac{Q_m^2}{2} + \sqrt{\frac{Q_m^4}{4} - 6Q_m^2|\bar{q}|}}$. There are a first and a second distinguishing masses $M_1 = \frac{1}{2}f(r_1)$ and $M_2 = \frac{1}{2}f(r_2)$. When $M < M_2$ there is one simple horizon. When $M = M_2$, there are one simple horizon and one double distant horizon. When $M_2 < M < M_1$ there are three simple horizons. When $M = M_1$ there are one double horizon and one simple distant horizon. When $M > M_1$ there is one simple distant horizon.

The second situation is displayed on panel (2b) of Fig. 2 and corresponds to the case when $\frac{24\bar{q}}{Q_m^2} = 1$. Now the maximum, minimum and inflexion points coincide. We have now only one distinguishing mass $M_{\rm t}$. When $M < M_{\rm t}$, there is one simple horizon. When $M = M_{\rm t}$ the horizon is triple. When $M > M_{\rm t}$, there is one simple distant horizon.

The third situation is displayed on panel (2c) of Fig. 2 and corresponds to the case when $\frac{24\bar{q}}{Q_m^2} > 1$. Here there are no extrema. There are no distinguishing masses, and there is one simple horizon.

B. The case $\bar{q} \geq 0$ and $\Lambda = 0$

The case $\bar{q} = 0$ is simple. Eqs. (59), (60), and (61) yield here

$$f(r) = r + \frac{Q_m^2}{r}\,, \tag{84}$$

$$-r^4 + Q_m^2 r^2 = 0\,, \tag{85}$$

$$r^2 = 0\,, \tag{86}$$

respectively. So $f(r)$ has no inflexion points and possesses one minimum at $r_{\rm min}=Q_m$. There is one distinguishing mass, $M_1 = \frac{1}{2}f(r_{\rm min}) = Q_m$. When $M < M_1$, there are no horizons. When $M = M_1$, we obtain one double horizon. When $M > M_1$, there are two simple horizons, see the sketch on panel (2d) of Fig. 2.

For the case $\bar{q} > 0$ and $\Lambda = 0$, Eqs. (59), (60), and (61) yield

$$f(r) = r + \frac{Q_m^2}{r} + \frac{2Q_m^2\bar{q}}{r^3}\,, \tag{87}$$

$$-r^4 + Q_m^2 r^2 + 6Q_m^2\bar{q} = 0\,, \tag{88}$$

$$r^2 + 12\bar{q} = 0\,, \tag{89}$$

respectively. Clearly, Eq. (89) has no real roots and thus there are no inflexion points. Eq. (88) has one real positive root $r_{\rm min}=\sqrt{\frac{Q_m^2}{2}+\sqrt{\frac{Q_m^4}{4}+6Q_m^2\bar{q}}}$, which gives the minimum of $f(r)$. Eq. (87) has asymptotic values $f(0)=\infty$ and $f(\infty)=\infty$. See the sketch on panel $(2d)$ of Fig. 2. As in the previous case $\bar{q}=0$ we can find zero, one double or two simples horizons.

VI. EXACT SOLUTIONS WITH A NEGATIVE COSMOLOGICAL CONSTANT, $\Lambda < 0$

The case $\Lambda < 0$ is subdivided into $\bar{q} < 0$ and $\bar{q} \geq 0$. All panels and plots for this $\Lambda < 0$ case are shown in Fig. 3.

A. The case $\bar{q} < 0$ and $\Lambda < 0$

Here, Eqs. (59), (60), and (61) yield

$$f(r) = \frac{|\Lambda| r^3}{3} + r + \frac{Q_m^2}{r} - \frac{2Q_m^2|\bar{q}|}{r^3}\,, \tag{90}$$

$$-|\Lambda| r^6 - r^4 + Q_m^2 r^2 - 6Q_m^2|\bar{q}| = 0\,, \tag{91}$$

$$|\Lambda| r^6 + Q_m^2 r^2 - 12Q_m^2|\bar{q}| = 0\,, \tag{92}$$

In this case the discriminant Δ in Eq. (69) is negative, thus, there is only one real root, say, Y_1, the other two roots Y_2 and Y_3 are conjugated complex numbers. Since the product $Y_1Y_2Y_3$ according to Eq. (70) is positive, the real root Y_1 should be positive. This means that there exists one real positive root $r_i=\sqrt{Y_1}$ and thus the function $f(r)$ has one inflexion point. Since $f(0) = -\infty$, $f(\infty) = +\infty$, the plots of the function $f(r)$ can be of the type $(3a)$, $(3b)$ or $(3c)$ of Fig. 3. All these three sketches have one inflexion point, and the difference between them is predetermined by the number of extrema, i.e., by the number of real positive roots of Eq. (91), X_1, X_2, X_3. Since the sum and the product of these quantities are negative (see Eq. (65)), there are three possibilities: only one real negative root, three negative real roots, and two positive real roots and one negative real root.

When the positive roots X_1 and X_2 do not coincide, one can find one maximum and one minimum, as on the sketch depicted on panel $(3a)$ of Fig. 3. When $X_1=X_2$, three points coincide: the maximum, minimum and inflexion point, see the sketch displayed on panel $(3b)$ of Fig. 3. In the first and second cases there are no extrema, and we obtain the sketch depicted on panel $(3c)$ of Fig. 3.

According to the sketches $(3a)$, $(3b)$, $(3c)$ the horizontal mass line can cross the plot of the function $f(r)$ once, two or three times. This means that this submodel can admit one simple horizon, three simple horizons, one triple horizon and two horizons, one of them being a double horizon. In other words, it is guarantied that there is at least one horizon in this model for any value of the mass M.

B. The case $\bar{q} \geq 0$ and $\Lambda < 0$

In the case $\bar{q} = 0$ Eqs. (59), (60), and (61) yield

$$f(r) = \frac{|\Lambda| r^3}{3} + r + \frac{Q_m^2}{r}\,, \tag{93}$$

$$r^2\left(-|\Lambda| r^4 - r^2 + Q_m^2\right) = 0\,, \tag{94}$$

$$r^2\left(|\Lambda| r^4 + Q_m^2\right) = 0\,, \tag{95}$$

respectively. Clearly, when $\Lambda < 0$, there are no inflexion points. There is only one extremum, a minimum given by $r_{\rm min}=\sqrt{\frac{1}{2|\Lambda|}\left(\sqrt{1+4Q_m^2|\Lambda|}-1\right)}$. Also $f(0)=+\infty$ and $f(\infty)=+\infty$. The plot of the function $f(r)$ has the form of the sketch displayed on panel $(3d)$ of Fig. 3. In this case one can find explicitly the critical value of the mass, $M_{\rm c}$. Using the equality $M_{\rm c} = \frac{1}{2}f(r_{\rm min})$ one finds

$$M_{\rm c} = \frac{1}{3}\left(r_{\rm min} + \frac{2Q_m^2}{r_{\rm min}}\right)\,. \tag{96}$$

When $M < M_{\rm c}$, the mass line does not cross the plot of $f(r)$, i.e., the corresponding object does not have horizons. When the mass exceeds the critical one, $M > M_{\rm c}$, the mass line crosses the plot twice, and two horizons appear. Finally, when $M=M_{\rm c}$, there is one double horizon.

In the case $\bar{q} > 0$ and $\Lambda < 0$, Eqs. (59), (60), and (61) yield

$$f(r) = \frac{|\Lambda| r^3}{3} + r + \frac{Q_m^2}{r} + \frac{2Q_m^2|\bar{q}|}{r^3}\,, \tag{97}$$

$$-|\Lambda| r^6 - r^4 + Q_m^2 r^2 + 6Q_m^2|\bar{q}| = 0\,, \tag{98}$$

$$|\Lambda| r^6 + Q_m^2 r^2 + 12Q_m^2|\bar{q}| = 0\,, \tag{99}$$

In this case the discriminant in Eq. (69) is negative and there is only one real root. Since the product of the roots is now negative, the real root is also negative. Thus, there are no real roots, and so there are no inflexion points. There exists a minimum of the function $f(r)$, since $f(0) = +\infty$ and $f(\infty) = +\infty$. The plot of this function $f(r)$ is depicted in panel $(3d)$ of Fig. 3. This model admits two simple or one double horizons. The horizons can disappear when the mass M is less than the critical mass, related to the minimal value of the function $f(r)$.

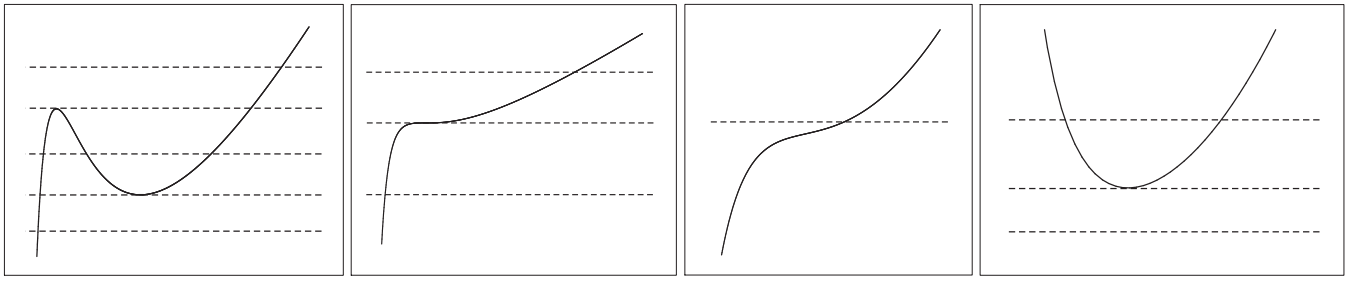

(3a) (3b) (3c) (3d)

FIG. 3: $\Lambda < 0$. Sketches of the auxiliary function $f(r)=-\frac{1}{3}\Lambda r^3+r+Q_m^2 r^{-1}+2Q_m^2\bar{q}r^{-3}$ for negative cosmological constant $\Lambda < 0$. At the points r_h, in which the horizontal mass line $y = 2M$ crosses the curve of the function $y = f(r)$, the metric function $N(r)$ takes zero values, i.e., the spheres $r = r_h$ are horizons. The plots on panels (3a), (3b), (3c) show typical cases for which $\bar{q} < 0$, and panel (3d) illustrates the cases for $\bar{q} \geq 0$. In panel (3a) the plot of the function $f(r)$ displays one inflexion point and two extrema. Depending on the mass M, and thus on the mass line $y = 2M$, one can find one, one double plus one simple, three simple, one simple plus one double, and one simple horizon. In the case the extrema coincide one has a quadruple horizon, not shown in panel. In panel (3b) the inflexion point coincides with an extremum. One can find one simple horizon. In the panel (3c) there is one inflexion point and no extrema. One can find one simple horizon. In panel (3d) there are no inflexion points and there is one extremum, a minimum. In this case there are zero, one double, and two simple horizons.

VII. SHORT RESUMÉ

In Table I we present a summary of the results of the classification of the five-parameter family of exact solutions with respect to number of horizons and their type, i.e., whether they are single, double, triple, or quadruple. We use in this table the following symbols: we write 0 when there are no horizons; 1s, 2s, 3s, and 4s means one, two, three, and four simple horizons, respectively; 1d and 2d to denote one and two double horizons, respectively; the symbol 1t to mean one triple horizon; and 1q to mean one quadruple horizon. We also use the following expressions: 1s+1d means that there are one simple and one double horizon; 2d+2d means two double horizons. The entries in the table are given by the nonminimal parameter $\bar{q}$ (for the cases $\bar{q} < 0$ and $\bar{q} \geq 0$) and the cosmological constant Λ (for the cases $\Lambda < 0$, $\Lambda = 0$, $0 < \Lambda < \Lambda_c$, $\Lambda = \Lambda_c$, and $\Lambda > \Lambda_c$), where Λ_c is the critical value of the cosmological constant $\Lambda_c \equiv \frac{Q_m^2}{972\bar{q}^2}$, see Eq. (71).

	$\Lambda < 0$	$\Lambda = 0$	$0 < \Lambda < \Lambda_c$	$\Lambda = \Lambda_c$	$\Lambda > \Lambda_c$
$\bar{q} < 0$	1s; 3s; 1t; 1s+1d	1s; 3s; 1t; 1s+1d	0; 1d; 2s; 2s+1d; 4s; 2d; 1s+1t; 1q	0; 1d; 2s; 1s+1t; 1q	0; 2s; 1d
$\bar{q} \geq 0$	0; 2s; 1d	0; 2s; 1d	1s; 1s+1d; 3s; 1t	1s; 1s+1d; 3s; 1t	1s; 1s+1d; 3s; 1t

TABLE I: The number of horizons in the five-parameter family of exact solutions as a function of the nonminimal parameter $\bar{q}$ and the cosmological constant Λ.

We have now completed the classification of the black holes and horizons existent in these spherical symmetric nonminimal models. We will give below two examples where this classification fits. These examples are typical cases for $\bar{q} < 0$ and $\bar{q} \geq 0$. They are the Drummond-Hathrell model and the regular black hole, respectively.

VIII. THE DRUMMOND-HATHRELL MODEL: EXAMPLE OF A NONMINIMAL THEORY WITH $\bar{q} < 0$

In [19], Drummond and Hathrell have investigated a model in which the parameters of the nonminimal coupling were calculated in the framework of the one-loop corrections to QED. These parameters are of the form $q_1 = -q$, $q_2 = \frac{13}{5}q$, $q_3 = -\frac{2}{5}q$, where $q = \frac{\alpha\lambda_e^2}{36\pi}$, λ_e being the Compton radius of electron. Clearly, for these Drummond-Hathrell parameters one obtains that $10q_1 + 4q_2 + q_3 = 0$, so it obeys Eq. (43) that we have assume from the start. Moreover $\bar{q} = -\frac{2}{5}q$, so $\bar{q} < 0$ and it falls in the case $\bar{q} < 0$ that we have treated before. Since $\bar{q}$ is given for a given q, the two nonminimal coupling constants, q and $\bar{q}$, reduce to one independent coupling constant, q, say. We deal with a four parameter model.

Thus, the Drummond-Hathrell model has

$$\sigma(r) = 1\,, \tag{100}$$

and the metric function $N(r)$ takes the form, see Eq. (48),

$$N(r) = 1 - \frac{\Lambda r^2}{3} + \frac{Q_m^2\left(1+\frac{2\Lambda q}{3}\right)r^2 - 2Mr^3 - \frac{14}{5}Q_m^2 q}{r^4 + 2Q_m^2 q}\,, \tag{101}$$

At the center the metric function $N(r)$ takes the value $N(0) = -2/5$. Now we study the cases $\Lambda > 0$, $\Lambda = 0$, $\Lambda < 0$, and describe new fine details of the horizon structure of the solutions using the different masses M of the object.

A. The case $\Lambda > 0$

1. The distinguishing masses

For $\Lambda > 0$ in the Drummond-Hathrell case the corresponding figures are given in panels $(1a)$ to $(1e)$ in Fig. 1. We are faced with 15 different submodels, see curves I-XV depicted in Fig. 4, see also Table I.

We distinguish these models with respect to the mass M of the object. The analysis is rich but intricate and is based on the introduction of the following specific values of the mass.

$M_{\rm N}$: We start with the mass $M_{\rm N}$ that distinguishes models with and without a Newtonian-type attraction zone. For this value of the mass the solutions of the two equations, $N'(r_{\rm N}) = 0$ and $N''(r_{\rm N}) = 0$, coincide, but $N(r_{\rm N}) \neq 0$, see curve III in Fig. 4.

M_1: The mass M_1 appears when the minimum of the curve $N(r)$ touches the axis $N = 0$, see curve V in Fig. 4. This means that the two equations, $N(r_1) = 0$ and $N'(r_1) = 0$ give coinciding solutions.

M_2: Similarly, the value M_2 is for the case when the distant maximum touches the line $N = 0$, see curve VII on Fig. 4.

M_3: Similarly, the value M_3 is for the case when the maximum closest to the center touches the line $N = 0$, see curve VIII in Fig. 4.

M_{1m}, M_{2m}, M_{3m}: When the distant maximum is higher than the maximum closest to the center the corresponding masses differ from M_1, M_2, M_3. In this case the corresponding masses are written as M_{1m}, M_{2m}, M_{3m}, respectively, where the additional index m, stands for modified. In panel (b) of Fig. 4 other curves could be drawn. We stick to drawing in this panel (b) only the curves that are qualitatively different from those of panel (a). These are curves X and XI only, which correspond to the masses M_{2m} and M_{3m}. The curve for the mass value M_{1m} is not displayed since it can be obtained as a deformed curve V from panel (a) of Fig. 4.

$M_2 = M_3$: When $M_2 = M_3$ we deal with a specific case depicted in panel (c), curve XIII, of Fig. 4.

$M_{\rm T1}$, $M_{\rm T2}$: There are also two specific sets of values of two parameters, the mass M and $\bar{q}$, for which three equations give the same roots, namely, $N(r_{\rm T}) = 0$, $N'(r_{\rm T}) = 0$ and $N''(r_{\rm T}) = 0$, where the subscript T is for triple. There are two masses that fulfill these conditions. One, $M_{\rm T1}$, is depicted in panel (d), curve XIV, of Fig. 4, and shows the case when the inner, Cauchy, and event horizons coincide. The other, $M_{\rm T2}$, is depicted in panel (e), curve XV, of Fig. 4, and shows the case when the Cauchy, event, and cosmological horizons coincide.

$M_{\rm Q}$: The last specific value of the mass, $M_{\rm Q}$, appears for a specific set $M_{\rm Q}$, $\bar{q}_{\rm Q}$, $\Lambda_{\rm Q}$, for which $N(r_{\rm Q}) = 0$, $N'(r_{\rm Q}) = 0$, $N''(r_{\rm Q}) = 0$, and $N'''(r_{\rm Q}) = 0$, see the panel (f), curve XV, of Fig. 4.

2. The fifteen cases

Now we comment the fifteen cases based on the plots of $N(r)$ as a function of r.

(1) $M = 0$

This case is shown in curve I of panel (a) of Fig. 4 and is related to the crossing of the line $(1a)$ on Fig. 1 with the line $M = 0$, the bottom horizontal line. This solution has a similar structure to the Schwarzschild-dS solution. $N(r)$ is characterized by a finite minimum at the center, an inner black hole zone and an inner event horizon, a trap between the horizon and the maximum, a zone of repulsion, a cosmological horizon, and a dS region.

(2) $0 < M < M_{\rm N}$

This case is shown in curve II of panel (a) of Fig. 4 and looks like the previous case $M = 0$. The difference is in the height of the maximum.

(3) $M = M_{\rm N}$

This case is shown in curve III of panel (a) of Fig. 4. It separates spacetimes with and without a Newtonian-type attraction zone. This solution has also a similar structure to the Schwarzschild-dS solution. $N(r)$ is characterized by a minimum at the center, an inner black hole zone, an inner event horizon, a trap between the horizon and the maximum, a zone of repulsion, a cosmological horizon, and a dS region.

(4) $M_{\rm N} < M < M_1$

This case is shown in curve IV of panel (a) of Fig. 4. The curve is characterized by a minimum at the center, an inner black hole zone, an inner event horizon, a trap between the horizon and the maximum, a zone of repulsion, a neutral zone, a Newtonian attraction zone, a zone of repulsion, a cosmological horizon, and a dS region.

(5) $M = M_1$

This case is shown in curve V of panel (a) of Fig. 4. There are three horizons, one of them is a double horizon. It can be thought of as extremal Reissner-Nordström-dS solution, with a Schwarzschild structure replacing the time-like singularity. The curve is characterized by a minimum at the center, an inner black hole zone, an inner black hole horizon, a trap between the horizon and the maximum, a zone of repulsion, a double extremal horizon, a Newtonian attraction zone, a zone of cosmological

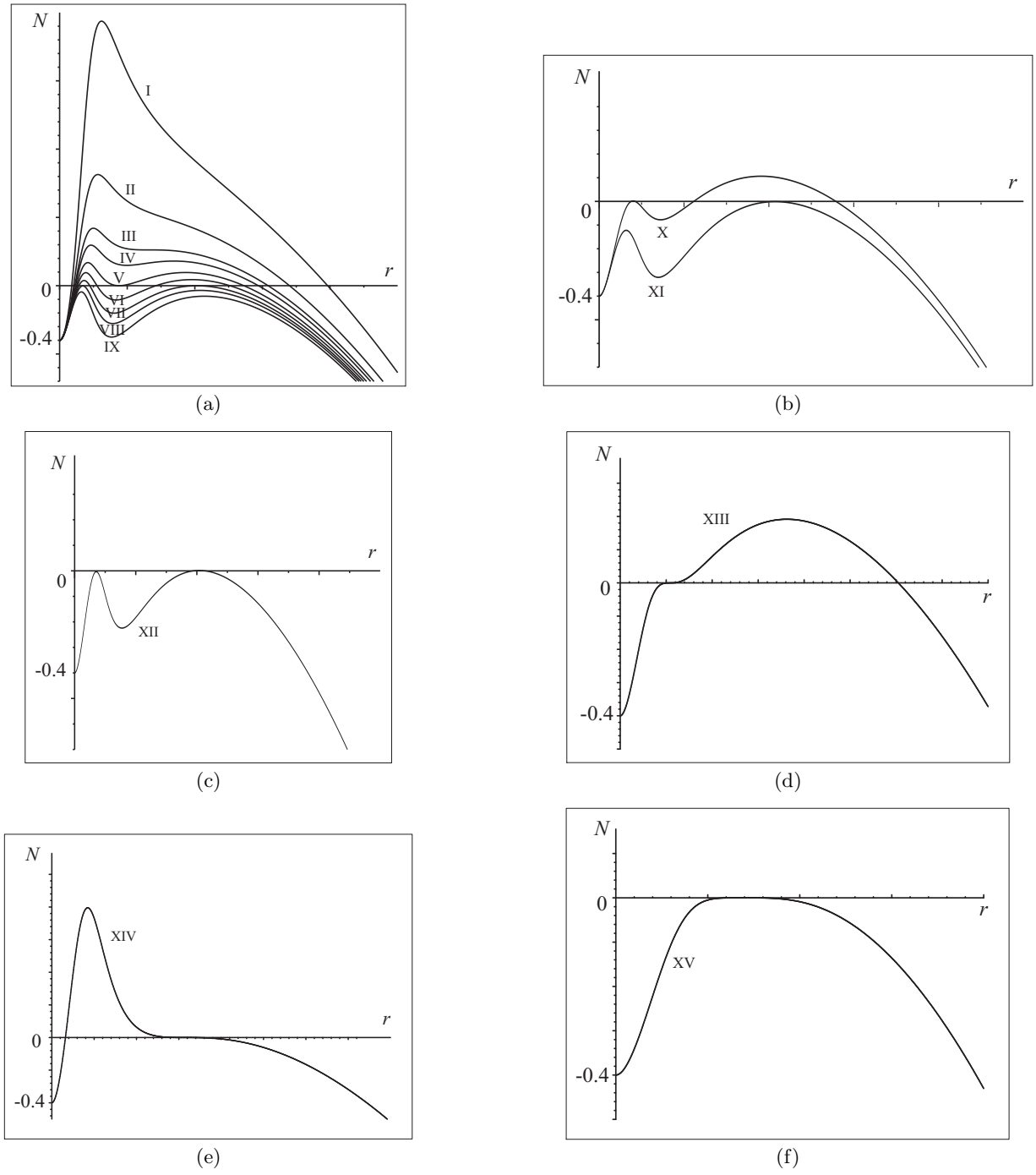

FIG. 4: Quasiregular nonminimal black holes of the Drummond-Hathrell type with $\Lambda > 0$. See text for details.

repulsion, a cosmological horizon, and a dS region. This case corresponds to the cross of the curve in panel $(1a)$ of Fig. 1, for which the horizontal mass line touches the minimum of the plot of the auxiliary function $f(r)$.

(6) $M_1 < M < M_2$

This case is shown in curve VI of panel (a) of Fig. 4. There are four horizons. It can be thought of as a Reissner-Nordström-dS solution, with a Schwarzschild structure replacing the timelike singularity. $N(r)$ is characterized by a minimum at the center, an inner black hole zone, an inner event horizon, a trap between the horizon and the maximum, a zone of repulsion, a Cauchy horizon, a second black hole zone, a second event horizon, a Newtonian attraction zone, a zone of cosmological repulsion, and a cosmological horizon, and a dS region. This case corresponds to the situation, for which the horizontal mass line crosses the plot of the auxiliary function in four different points, see panel $(1a)$ of Fig. 1.

(7) $M = M_2$
This case is shown in curve VII of panel (a) of Fig. 4. There are three horizons, one of them is a double horizon. It can be thought of as Reissner-Nordström-dS solution, where the second event horizon coincides with the cosmological horizon, and with a Schwarzschild structure replacing the timelike singularity. The curve is characterized by a minimum at the center, an inner black hole zone, an inner black hole horizon, a small trap between the horizon and the maximum, a zone of repulsion, a Cauchy horizon, a second black hole zone, a double horizon where the second event horizon coincides with the cosmological horizon, and a dS region. This case corresponds to the situation for which the horizontal mass line touches the plot of the auxiliary function in the right maximum see panel (1a) of Fig. 1.
(8) $M = M_3$
This case is shown in curve VIII of Fig. 4. This solution can be thought of as a limiting Kasner type solution $N(r)$ is always negative, apart at one point where it is zero. This case corresponds to the situation, for which the horizontal mass line touches the plot of the auxiliary function in the left maximum, see panel (1a) of Fig. 1.
(9) $M > M_3$
This case is shown in curve IX of Fig. 4. This solution can be thought of as a Kasner type solution $N(r)$ is always negative. There are no horizon. This case corresponds to the situation, for which the horizontal mass line is situated above the plot of the auxiliary function, see panel (1a) of Fig. 1.
(10) $M = M_{3m}$
This case is shown in curve X of panel (b) of Fig. 4. It is a new case. There are three horizons, one is a double horizon, the inner event horizon and the Cauchy horizon coincide. It can be thought as having the same structure of the Reissner-Nordström-dS solution. For this case the curve has a minimum at the center, an inner black hole Reissner-Nordström zone, a double horizon where the inner event horizon and the Cauchy horizon coincide, a second black hole zone, outer horizon, a Newtonian attraction zone, a zone of cosmological repulsion, a cosmological horizon, and a dS region.
(11) $M = M_{2m}$
This case is shown in curve XI of panel (b) of Fig. 4. It is a limiting Kasner type solution.
(12) $M = M_{2m} = M_{3m}$
This case is shown in curve XII of panel (c) of Fig. 4. It is also a limiting Kasner type solution.
(13) $M = M_{\rm T1}$
This case is shown in curve XIII of panel (d) of Fig. 4. This solution has also a similar structure to the Schwarzschild-dS solution. For this case there is a minimum at the center, a triple inner, Cauchy and outer horizons, a Newtonian attraction zone, a zone of cosmological repulsion, a cosmological horizon, and a dS region.
(14) $M = M_{\rm T2}$
This case is shown in curve XIV of panel (e) of Fig. 4. This solution has also a similar structure to the Schwarzschild-dS solution. For this case there is a minimum at the center, an inner black hole zone, an inner event horizon, a trap, a zone of repulsion, triple horizon where the Cauchy, the second event, and the cosmological horizons coincide, and a dS region. This situation corresponds to the case, when the horizontal mass line crosses the plot of the auxiliary function in the triple point depicted on panel (1c) of Fig.1.
(15) $M = M_{\rm Q}$
This case is shown in curve XV of panel (e) of Fig. 4. It is also a limiting Kasner type solution. This situation corresponds to the case, when the horizontal mass line crosses the plot of the auxiliary function in the quadruple point depicted on panel (1d) of Fig.1.

With the features given above one can sketch with some ease the corresponding Carter-Penrose diagrams.

B. The case $\Lambda = 0$

1. The distinguishing masses

For $\Lambda = 0$ in the Drummond-Hathrell case the corresponding figures are given in panels (1a) to (1c) in Fig. 2. We have 7 different submodels, see curves I-VII depicted in Fig. 5, see also Table I.

For $\Lambda = 0$ the spacetime is asymptotically Minkowskian, i.e., $N(r) \to 1$ at $r \to \infty$. All the curves have a minimum at the center with $N(0) = -\frac{2}{5}$, an inner black hole zone, and an inner event horizon.

There are two distinguishing masses, M_1 and M_2. The mass M_1 is related to the case when curve III on panel (a) of Fig. 5 touches the axis $N = 0$ in its minimum. The mass M_2 corresponds to the case when curve V of Fig. 5 touches this axis in its maximum. There are seven intrinsic cases distinguished according to different values of the mass M.

2. The seven cases

(1) $M = 0$
This case is shown in curve I of panel (a) of Fig. 5 and is related to the crossing of the line (2a) on Fig. 2 with the line $M = 0$, the bottom horizontal line. $N(r)$ is characterized by a finite minimum at the center, an inner black hole zone, an inner event horizon, a trap between the horizon and the maximum, a zone of repulsion and an asymptotic flat region. This case corresponds to the cross of the curve in panel (2a) of Fig. 2, for which the bottom horizontal mass line crosses $f(r)$.
(2) $0 < M < M_1$
This case is shown in curve II of panel (a) of Fig. 5. The curve is characterized by a minimum at the center, an inner black hole zone, an inner event horizon, a trap between the horizon and the maximum, a zone of repulsion, a neutral zone, a Newtonian attraction zone, and an asymptotic flat region. As in the previous case, this

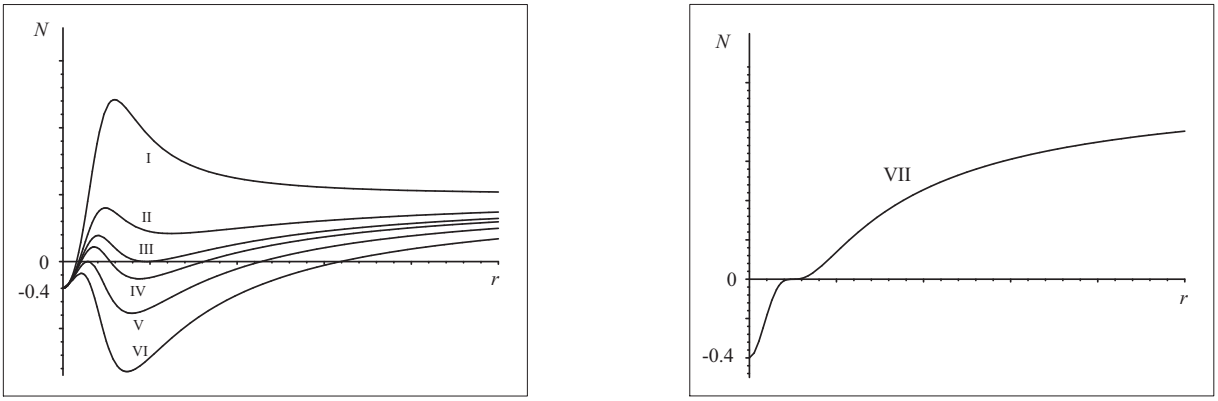

FIG. 5: Quasi-regular nonminimal black holes of the Drummond-Hathrell type with $\Lambda = 0$. See text for details.

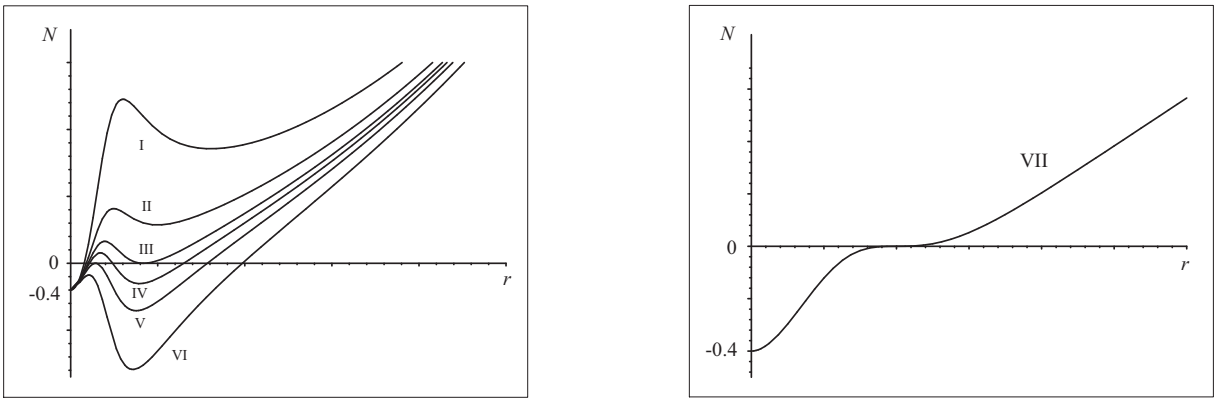

FIG. 6: Quasi-regular nonminimal black holes of the Drummond-Hathrell type with $\Lambda < 0$. See text for details.

case corresponds to the cross of the curve in panel (2a) of Fig. 2, for which the bottom horizontal mass line crosses $f(r)$.

(3) $M = M_1$

This case is shown in curve III of panel (a) of Fig. 5. There are two horizons, one of them is a double horizon. It can be thought of as extremal Reissner-Nordström solution, with a Schwarzschild structure replacing the Reissner-Nordström timelike singularity. The curve is characterized by a minimum at the center, an inner black hole zone, an inner black hole horizon, a trap between the horizon and the maximum, a zone of repulsion, a double extremal horizon, a Newtonian attraction zone, and an asymptotic flat region. This case corresponds to the cross of the curve in panel (2a) of Fig. 2, for which the horizontal mass line touches the minimum of the plot of the auxiliary function $f(r)$.

(4) $M_1 < M < M_2$

This case is shown in curve IV of panel (a) of Fig. 5. There are three horizons. It can be thought of as a Reissner-Nordström solution, with a Schwarzschild structure replacing the Reissner-Nordström timelike singularity. $N(r)$ is characterized by a minimum at the center, an inner black hole zone, an inner event horizon, a trap between the horizon and the maximum, a zone of repulsion, a Cauchy horizon, a second black hole zone, a second event horizon, a Newtonian attraction zone, and an asymptotic flat region. This case corresponds to the situation, for which the horizontal mass line crosses the plot of the auxiliary function in three different points, see panel (2a) of Fig. 2.

(5) $M = M_2$

This case is shown in curve V of panel (a) Fig. 5. There are two horizons, one of them is double. The curve is characterized by a minimum at the center, an inner black hole zone, a double horizon, in which an inner and a Cauchy horizons coincide, a second black hole zone, a second event horizon, a Newtonian attraction zone, and an asymptotic flat region. This case corresponds to the situation for which the horizontal mass line touches the plot of the auxiliary function in the maximum see the panel (2a) of Fig. 2.

(6) $M > M_2$

This case is shown in curve VI of Fig. 5. The curve is

characterized by a minimum at the center, a united black hole zone, an event horizon, a Newtonian attraction zone, and an asymptotic flat region. This case corresponds to the situation for which the horizontal mass line is situated above the maximum of the auxiliary function, see panel (2a) of Fig. 2, or crosses the line depicted on panel (2b) of Fig. 2.

(7) $M = M_1 = M_2$

This case is shown in curve VII of panel (b) of Fig. 5. One has one triple horizon, where the inner, Cauchy, and event horizons coincide. The curve is characterized by a minimum at the center, an inner black hole zone, a triple horizon, a Newtonian attraction zone, and an asymptotic flat region. This case corresponds to the situation for which the horizontal mass line crosses the plot of the auxiliary function in the triple point, see panel (2c) of Fig. 2.

With the features given above one can sketch with some ease the corresponding Carter-Penrose diagrams.

C. The case $\Lambda < 0$

1. The distinguishing masses

From the point of view of horizon structure and description, the case with negative cosmological constant, $\Lambda < 0$, does not differ qualitatively from the case $\Lambda = 0$. There are two masses M_1 and M_2 as in the $\Lambda = 0$ case.

2. The seven cases

We draw seven subcases illustrated by curves I-VI on panel (a) of Fig. 6 and by curve VII on panel (b) of Fig. 6. The main difference to the $\Lambda = 0$ case is that all the curves are asymptotically anti-de Sitter instead of asymptotically flat. The details are similar to the ones for the case $\Lambda = 0$.

With the features given above one can sketch with some ease the corresponding Carter-Penrose diagrams.

IX. THE REGULAR BLACK HOLE: EXAMPLE OF A NONMINIMAL THEORY WITH $\bar{q} \geq 0$

If we want regular solutions at the center then we have to impose further $N(0) = 1$ and $N'(0) = 0$. From Eq. (49) we see this happens when

$$\bar{q} = q\,. \tag{102}$$

Since we assume $q > 0$, see Eq. (50), the regular solutions fall in the case $\bar{q} \geq 0$, the case $\bar{q} = 0$ being a limiting case. In addition, the requirement given in Eq. (102), restrict the number of the two nonminimal coupling constants, q and $\bar{q}$, to just one independent coupling constant, q, say. We deal with a four parameter model.

Then the solution to Eq. (48) is of the form

$$N = 1 + \left(1 + \frac{2Q_m^2 q}{r^4}\right)^{-1} \left(-\frac{2M}{r} + \frac{Q_m^2}{r^2} - \frac{\Lambda}{3} r^2\right). \tag{103}$$

The four parameters in this family of exact solution are them q, M, Q_m, and Λ. Near the center the metric function $N(r)$ behaves as $N(r) = 1 + \frac{r^2}{2q} - \frac{Mr^3}{Q_m^2 q} + \ldots$, such that $N(0) = 1$, $N'(0) = 0$ and $N''(0) = \frac{1}{q}$. This means that the point $r = 0$ is a minimum of the regular function $N(r)$ independently of the sign and value of the cosmological constant Λ, and independently of the mass value M. Since $N(0) = 1$, the curvature scalar is regular in the center: $R(0) = \frac{6}{q}$. The quadratic scalar $R_{mn}R^{mn} = \frac{9}{q^2}$, and other curvature invariants are also finite in the center. Thus the spacetime is regular at the center. All the corresponding objects found within this solution are regular objects. The most important feature of the family of exact solutions is that it has solutions with horizons, i.e., regular black holes, depending on the relative values of the parameters. These solutions have been displayed in detail in [30], below we give a brief account of them.

A. The case $\Lambda > 0$

For $\Lambda > 0$, there are two critical masses M_{c1} and M_{c2}. Depending on the values of the parameters, the black hole solution can have three horizons, the Cauchy horizon, the event horizon and the cosmological horizon. When $M < M_{c1}$, there is one horizon only which is a cosmological horizon. A typical profile of the metric function $N(r)$ contains a central small cavity, a repulsion barrier, a zone of rest near the point of minimum, a Newtonian-type attraction zone with the potential going as $1/r$, a cosmological acceleration zone, and a asympotically dS zone. When $M = M_{c1}$, there is an extremal horizon that is double, formed by the Cauchy and event horizons, and there is a cosmological horizon. When $M_{c1} < M < M_{c2}$ there are three separate horizons, the Cauchy, event and cosmological horizons. When $M = M_{c2}$, there is a Cauchy horizon, and there is a double horizon, the event horizon and the cosmological horizon coincide. In this case the black hole is a cosmological supermassive regular extremal black hole. The whole visible universe is swallowed by this supermassive object. For $M > M_{c2}$ the Cauchy horizon becomes a cosmological horizon, the black hole is ultramassive. In such a universe there is only one horizon, which is cosmological, together with a repulsion region. This ultramassive black hole is of a new type, the three horizons coincide: the Cauchy, event and the cosmological horizons. There is further the case in which the three horizons coincide when $M_{c1} = M_{c2}$. With the features given above one can sketch the corresponding Carter-Penrose diagrams. For further details see [30].

B. The case $\Lambda = 0$

For $\Lambda = 0$ spacetime is asymptotically flat. Depending on the parameters, the black hole solution can have two horizons, the Cauchy horizon and the event horizon. When the mass is below a certain critical mass $M_{\rm c}$ there are no horizons. There is a double horizon when $M = M_{\rm c}$, and when $M > M_{\rm c}$ the Cauchy horizon and event horizons stand alone. With the features given above one can sketch the corresponding Carter-Penrose diagrams. For further details see [30].

C. The case $\Lambda < 0$

For $\Lambda < 0$ spacetime is asymptotically dS, and there is no cosmological horizon. Depending on the values of the parameters, the solution can have the Cauchy horizon and the event horizons. The critical mass $M_{\rm c}$ is a mass below which there are stars and above which there are regular black holes with the two horizons. When $M = M_{\rm c}$ the black hole has a double extremal horizon. With the features given above one can sketch the corresponding Carter-Penrose diagrams. For further details see [30].

X. CONCLUSIONS

In this work we have found a general exact spacetime solution for a Wu-Yang magnetic monopole in a nonminimal Einstein-Yang-Mills theory. This general solution is in fact a family of solutions with six parameters and they generically represent objects that go from bare magnetic monopoles to black holes with magnetic charge and several different types of horizons.

By a judicious choice we have reduced the number of parameters of the solution from six to five. Indeed imposing that the singularities at the center are spherical conical singularities, we have reduced the number of nonminimal parameters from three to two, q and $\bar{q}$. The other three parameters are the cosmological constant Λ, the Wu-Yang magnetic charge represented by Q_m, and the mass M.

We have provided a complete classification of these families of magnetic monopole solutions with respect to the number of horizons and their type. The important parameters in this classification are $\bar{q}$, Q_m, and Λ, together with the mass M of the spacetime. These furnish if there are zero, one, two, three, or four horizons, and whether they have a simple, double, triple, or quadruple degeneracy. The distinct horizons that appear within these families of objects are inner, Cauchy, event horizons, as well as a cosmological horizon when Λ is positive.

The objects have a great deal of unsuspected structure. They have a trapping parabolic region near the center controlled by the nonminimal parameters q and $\bar{q}$. The point $r = 0$ is an equilibrium point for which $N'(0) = 0$. When $\bar{q} > 0$, $N(0) > 0$, while for $\bar{q} < 0$ one has $N(0) > 0$, and so in this case the there is an inner horizon at a small positive r. For $\bar{q} = 0$ the horizon is at $r = 0$, and so the horizon and the conical singularity mesh in a null singular horizon. There is then a repulsion barrier contiguous to the nonminimal trap. Cauchy horizon and event horizons can then also appear, and in the positive cosmological constant case a cosmological dS horizon appears.

These general features of the families of exact solutions have been worked out for two special cases, the Drummond-Hathrell model and the regular black holes, examples of $\bar{q} < 0$ and $\bar{q} > 0$, respectively.

It will be certainly interesting to find magnetic monopole black hole solutions with an ansatz different from the Wu-Yang ansatz. These solutions would give nonminimal black holes and monopoles with Yang-Mills hair.

Acknowledgments

ABB and AEZ thank financial support from the Program of Competitive Growth of Kazan Federal University (KFU) Project No. 0615/06.15.02302.034 and from the Russian Foundation for Basic Research Grant (RFBR) No. 14-02-00598. ABB acknowledges financial support provided under the European Union's H2020 ERC Consolidator Grant "Matter and strong-field gravity: New frontiers in Einstein's theory", Grant No. MaGRaTh646597. JPSL thanks Fundação para a Ciência e Tecnologia (FCT) - Portugal for financial support through Project No. PEst-OE/FIS/UI0099/2014.

[1] J. B. Griffiths and J. Podolský, *Exact spacetimes in Einstein's General Relativity* (Cambridge University Press, Cambridge, 2009).
[2] R. Bartnik and J. McKinnon, "Particlelike solutions of the Einstein-Yang-Mills equations", Phys. Rev. Lett **61**, 141 (1988).
[3] P. Bizoń, "Colored black holes", Phys. Rev. Lett. **64**, 2844 (1990).
[4] P. Breitenlohner, P. Forgács, and D. Maison, "Gravitating monopole solutions", Nucl. Phys. B **383**, 357 (1992).
[5] M. Ortiz, "Curved-space magnetic monopoles" Phys. Rev. D **45**, R2586 (1992).
[6] K. Lee, V. P. Nair, and E. J. Weinberg, "Black holes in magnetic monopoles", Phys. Rev. D **45**, 2751 (1992).
[7] M. Wirschins, A. Sood, and J. Kunz, "Non-Abelian Einstein-Born-Infeld black holes", Phys. Rev. D **63**, 084002 (2001); arXiv:hep-th/0004130.
[8] M. Huebscher, P. Meessen, T. Ortín, and S. Vaula, "N=2 Einstein-Yang-Mills's BPS solutions", JHEP **0809**, 099 (2008); arXiv:0806.1477 [hep-th].

[9] J. M. Bardeen, "Non-singular general-relativistic gravitational collapse", in *Abstracts of the 5th International Conference on Gravitation and the Theory of Relativity*, edited by V. A. Fock et al. (Tbilisi University Press, Tbilisi, 1968), p. 174.

[10] E. Ayón-Beato and A. García, "The Bardeen model as a nonlinear magnetic monopole", Phys. Lett. B **493**, 149 (2000); arXiv:gr-qc/0009077.

[11] J. P. S. Lemos and V. T. Zanchin, "Regular black holes: Electrically charged solutions, Reissner-Nordström outside a de Sitter core", Phys. Rev. D **83**, 124005 (2011); arXiv:1104.4790 [gr-qc].

[12] S. V. Bolokhov, K. A. Bronnikov, M. V. Skvortsova, "Magnetic black universes and wormholes with a phantom scalar", Classical Quantum Gravity **29**, 245006 (2012); arXiv:1208.4619 [gr-qc].

[13] M.-S. Ma, "Magnetically charged regular black hole in a model of nonlinear electrodynamics", Ann. Phys. (N.Y.) **362**, 529 (2015); arXiv:1509.05580 [gr-qc].

[14] M. S. Volkov, N. Straumann, G. Lavrelashvili, M. Heusler, and O. Brodbeck, "Cosmological analogues of the Bartnik-McKinnon solutions", Phys. Rev. D **54**, 7243 (1996); arXiv:gr-qc/9605089 [gr-qc].

[15] E. Winstanley, "Existence of stable hairy black holes in $\mathfrak{su}(2)$ Einstein-Yang-Mills theory with a negative cosmological constant", Class. Quantum Grav. **16**, 1963 (1999); arXiv:gr-qc/9812064 [gr-qc].

[16] J. Bjoraker and Y. Hosotani, "Stable monopole and dyon solutions in the Einstein-Yang-Mills theory in asymptotically anti-de Sitter Space", Phys. Rev. Lett. **84**, 1853 (2000); arXiv:gr-qc/9906091.

[17] J. Bjoraker and Y. Hosotani, "Monopoles, dyons and black holes in the four-dimensional Einstein-Yang-Mills Theory", Phys. Rev. D **62**, 043513 (2000); arXiv:hep-th/0002098.

[18] A. R. Prasanna, "A new invariant for electromagnetic fields in curved space-time", Phys. Lett. A **37**, 331 (1971).

[19] I. T. Drummond and S. J. Hathrell, "QED vacuum polarization in a background gravitational field and its effect on the velocity of photons", Phys. Rev. D **22**, 343 (1980).

[20] A. B. Balakin and J. P. S. Lemos, "Non-minimal coupling for the gravitational and electromagnetic fields: A general system of equations", Class. Quantum Grav. **22**, 1867 (2005); arXiv:gr-qc/0503076.

[21] G. W. Horndeski, "Static spherically symmetric solutions to a system of generalized Einstein-Maxwell field equations", Phys. Rev. D **17**, 391 (1978).

[22] G. W. Horndeski, "Birkhoff's theorem and magnetic monopole solutions for a system of generalized Einstein-Maxwell field equations", J. Math. Phys. **19**, 668 (1978).

[23] F. Müller-Hoissen and R. Sippel, "Spherically symmetric solutions of the nonminimally coupled Einstein-Maxwell equations", Class. Quantum Grav. **5**, 1473 (1988).

[24] A. B. Balakin, V. V. Bochkarev, and J. P. S. Lemos, "Non-minimal coupling for the gravitational and electromagnetic fields: black hole solutions and solitons", Phys. Rev. D **77**, 084013 (2008); arXiv:0712.4066 [gr-qc].

[25] A. B. Balakin, J. P. S. Lemos, and A. E. Zayats, "Non-minimal coupling for the gravitational and electromagnetic fields: Traversable electric wormholes", Phys. Rev. D **81**, 084015 (2010); arXiv:1003.4584 [gr-qc].

[26] A. B. Balakin and A. E. Zayats, "Non-minimal Wu-Yang monopole", Phys. Lett. B **644**, 294 (2007); arXiv:gr-qc/0612019 [gr-qc].

[27] A. B. Balakin, H. Dehnen, and A. E. Zayats, "Non-minimal Einstein-Yang-Mills-Higgs theory: Associated, color and color-acoustic metrics for the Wu-Yang monopole model", Phys. Rev. D **76**, 124011 (2007); arXiv:0710.5070 [gr-qc].

[28] A. B. Balakin, S. V. Sushkov, and A. E. Zayats, "Non-minimal Wu-Yang wormhole", Phys. Rev. D **75**, 084042 (2007); arXiv:0704.1224 [gr-qc].

[29] A. B. Balakin and A. E. Zayats, "Dark energy fingerprints in the nonminimal Wu-Yang wormhole structure", Phys. Rev. D **90**, 044049 (2014); arXiv:1408.0862 [gr-qc].

[30] A. B. Balakin, J. P. S. Lemos, and A. E. Zayats, "Regular nonminimal magnetic black holes in spacetimes with a cosmological constant", Phys. Rev. D **93**, 024008 (2016); arXiv:1512.02653 [gr-qc].